AD-A078 367 DAVID W TAYLOR NAVAL SHIP RESEARCH AND DEVELOPMENT CE--ETC F/G 20/4
PARAMETRIC ANALYSIS OF CLOSE COUPLED CANARD TRANSONIC AERODYNAM--ETC(U)
MAY 77 J OTTENSOSER

UNCLASSIFIED DTNSRDC/ASED-399 NL

| OF |
ADA
078367

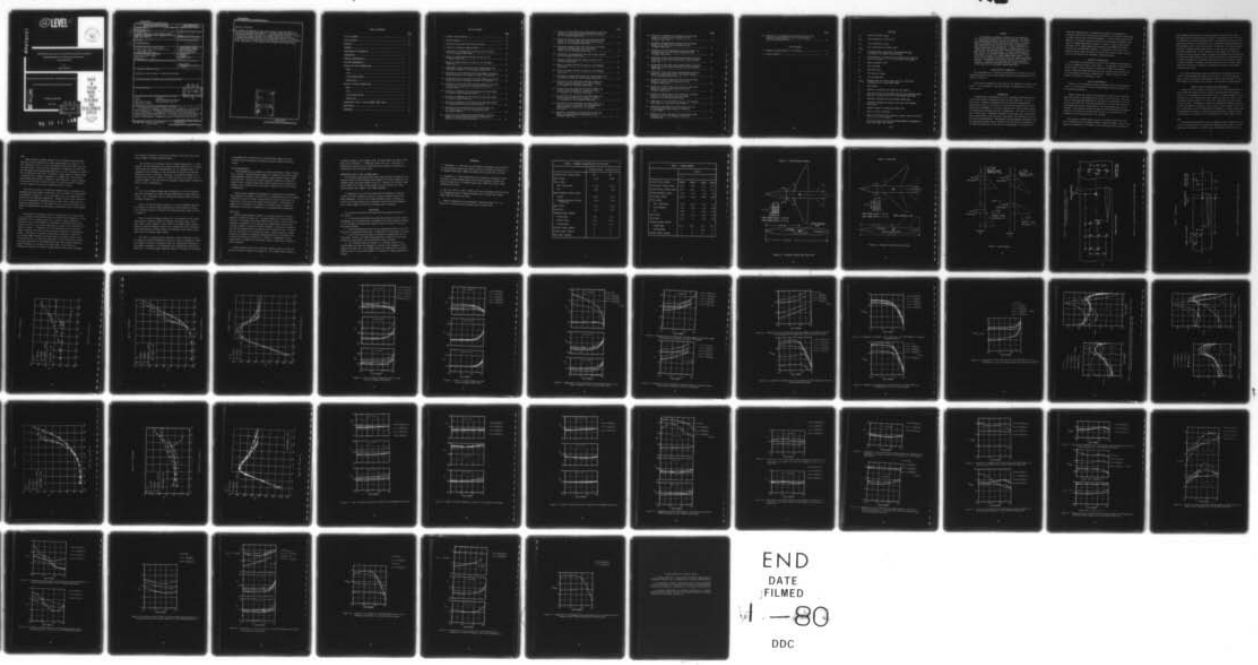

END
DATE
FILMED
1-80
DDC

(12) LEVEL II

PARAMETRIC ANALYSIS OF CLOSE COUPLED CANARD TRANSONIC AERODYNAMICS FOR A GENERALIZED WING-BODY CONFIGURATION

by

Jonah Ottensoser

AVIATION AND SURFACE EFFECTS DEPARTMENT

DTNSRDC ASED-399

May 1977

DAVID W. TAYLOR NAVAL SHIP RESEARCH AND DEVELOPMENT CENTER

BETHESDA
MARYLAND
20084

UNCLASSIFIED

SECURITY CLASSIFICATION OF THIS PAGE *(When Data Entered)*

REPORT DOCUMENTATION PAGE	READ INSTRUCTIONS BEFORE COMPLETING FORM
1. REPORT NUMBER: DTNSRDC/ASED-399	2. GOVT ACCESSION NO. / 3. RECIPIENT'S CATALOG NUMBER
4. TITLE *(and Subtitle)*: PARAMETRIC ANALYSIS OF CLOSE COUPLED CANARD TRANSONIC AERODYNAMICS FOR A GENERALIZED WING-~~BODY~~ CONFIGURATION	5. TYPE OF REPORT & PERIOD COVERED: Final rept.
	6. PERFORMING ORG. REPORT NUMBER
7. AUTHOR(s): Jonah Ottensoser	8. CONTRACT OR GRANT NUMBER(s): 12 63
9. PERFORMING ORGANIZATION NAME AND ADDRESS: David W. Taylor Naval Ship Research and Development Center, Bethesda, Maryland 20084	10. PROGRAM ELEMENT, PROJECT, TASK AREA & WORK UNIT NUMBERS: Program Element 62754N, Task Area WF1421706, Work Unit 1650-123
11. CONTROLLING OFFICE NAME AND ADDRESS: Naval Air Systems Command, NAVAIR 320D, Washington, D.C. 20361	12. REPORT DATE: May 1977
	13. NUMBER OF PAGES: 60
14. MONITORING AGENCY NAME & ADDRESS *(if different from Controlling Office)*	15. SECURITY CLASS. *(of this report)*: UNCLASSIFIED
	15a. DECLASSIFICATION/DOWNGRADING SCHEDULE

16. DISTRIBUTION STATEMENT *(of this Report)*

APPROVED FOR PUBLIC RELEASE: DISTRIBUTION UNLIMITED

17. DISTRIBUTION STATEMENT *(of the abstract entered in Block 20, if different from Report)*

18. SUPPLEMENTARY NOTES

DDC RECEIVED DEC 17 1979 B

19. KEY WORDS *(Continue on reverse side if necessary and identify by block number)*

Buffet
Canards
Close Couple Canards
High Angle of Attack
Transonic
Buffet Measurement Technique
High Performance Aircraft

20. ABSTRACT *(Continue on reverse side if necessary and identify by block number)*

An experimental parametric analysis has been completed for close-coupled canard effects on the transonic aerodynamics of a generalized wing-body aircraft configuration. The parameters investigated include wing sweep and position and deflection and planform of the canard for aircraft configurations with horizontal tail on and tail off. It was found that a 45-degree delta canard at approximately -5-degrees deflection, located above and forward of

(Continued on reverse side)

DD FORM 1 JAN 73 1473 EDITION OF 1 NOV 65 IS OBSOLETE S/N 0102-LF-014-6601

UNCLASSIFIED

SECURITY CLASSIFICATION OF THIS PAGE *(When Data Entered)*

387 695

(Block 20 continued)

but slightly overlapping the wing, gave the best overall performance. A canard placed properly with respect to a 50-degree sweep wing resulted in aerodynamic performance suitable for a highly maneuverable fighter. Further, a close-coupled canard used with the 25-degree sweep wing resulted in aerodynamic performance desirable for attack/bomber missions. In addition, it was found that a properly placed canard was useful in alleviating aircraft buffet, particularly on the wing with the 50-degree leading edge sweep.

TABLE OF CONTENTS

LIST OF FIGURES

LIST OF TABLES

NOTATION

C_D	Drag coefficient, D/qS_w
C_{D_o}	Drag coefficient at zero lift
C_L	Lift coefficient, L/qS_w
$C_{L_{BO}}$	Lift coefficient for buffet onset
C_M	Pitching moment coefficient, Pitching Moment/$qS_w\bar{c}$; see Figure 1 for moment reference point
C_i	Identification of canards tested; subscript "i" takes on values of either 0, 1, 2 or 3; see Table 2 and Figure 2
$\bar{c}$	Mean aerodynamic chord
D	Drag in pounds
H_T	Horizontal tail
L	Lift force in pounds
L/D	Lift-to-drag ratio
L/D_{max}	Maximum value of lift-to-drag ratio for a particular configuration at a given Mach number
M	Mach number
P_j	Canard or horizontal tail position; see Figure 3
S_w	Wing area; equal to 2.05 square feet for the 25-degree sweep wing and 2.11 square feet for the 50-degree sweep wing
S_3	Indicates fuselage with the 25-degree sweep wing
S_4	Indicates fuselage and vertical tail with the 50-degree sweep wing
q	Dynamic pressure in pounds per square foot
α	Angle of attack in degrees
δ	Canard or horizontal tail deflection angle; values are either -10, -5, 0, 5 or 10 degrees
σ	Root mean square value of wing bending moment as measured by wing strain gage; see Figure 4

ABSTRACT

An experimental parametric analysis has been completed for close-coupled canard effects on the transonic aerodynamics of a generalized wing-body aircraft configuration. The parameters investigated include wing sweep and position and deflection and planform of the canard for aircraft configurations with horizontal tail on and tail off. It was found that a 45-degree delta canard at approximately -5-degrees deflection, located above and forward of but slightly overlapping the wing, gave the best overall performance. A canard placed properly with respect to a 50-degree sweep wing resulted in aerodynamic performance suitable for a highly maneuverable fighter. Further, a close-coupled canard used with the 25-degree sweep wing resulted in aerodynamic performance desirable for attack/bomber missions. In addition, it was found that a properly placed canard was useful in alleviating aircraft buffet, particularly on the wing with the 50-degree leading edge sweep.

ADMINISTRATIVE INFORMATION

The investigation was funded and authorized by the Naval Air Systems Command (AIR-320D) under Program Element 627S4N, Task Area WF1421706, and Work Unit 1650-123.

This work was completed in 1972 prior to the adoption of a metric unit policy. In the interest of time and economy, no conversion was made to metric units.

INTRODUCTION

A comprehensive investigation into the aerodynamic characteristics of close-coupled canard configured aircraft has been completed. As part of this effort, transonic aerodynamic data were generated experimentally (References 1 and 2) in the David W. Taylor Naval Ship Research and Development Center (DTNSRDC) 7- by 10-Foot Transonic Wind Tunnel using a model of a generalized wing-body aircraft configuration. This report is an analysis of these data. Parameters evaluated include wing sweep, canard planform, canard position and deflection, Mach number, and horizontal tail-off and tail-on configurations. Measurements include standard aerodynamic data and wing bending moment data to determine the aerodynamic performance and the buffeting qualities of the aircraft configurations. An analysis of

these data indicates that a 45-degree delta canard at approximately -5-degrees deflection, located above and forward of but slightly overlapping the wing, gave the best overall performance. A canard placed properly with respect to a 50-degree sweep wing resulted in aerodynamic performance suitable for a highly maneuverable fighter. Further, a close-coupled canard used with the 25-degree sweep wing resulted in aerodynamic performance desirable for attack/bomber missions. In addition, it was found that a properly placed canard was useful in alleviating aircraft buffet, particularly on the wing with the 50-degree leading edge sweep.

AIRCRAFT CONFIGURATIONS

The geometric characterisitcs of the 25- and 50-degree wing sweep aircraft are presented in Table 1 and Figure 1. The geometric characteristics of the various canard planforms are presented in Table 2 and Figure 2. Figure 3 shows the canard and horizontal tail location variations for the 25- and 50-degree sweep wing configurations. Further details of these models are provided in References 1 and 2.

DATA AND MEASUREMENTS

Details of the experimental tunnel conditions are given in References 1 and 2. A description of the wing bending moment setup is presented in the following paragraphs.

Figure 4 shows the wing-root bending gages located on the 40-percent chord line which is approximately the elastic axis of the wing. The location of these gages was determined by the point of intersection of the 40-percent chord line and a line drawn perpendicular to this chord line passing through the point of intersection of the wing trailing edge and the fuselage. This procedure placed the gage on the most inboard line perpendicular to the elastic axis where this line was not constrained in its movements by the intersection with the fuselage.

The wing-root bending gages on each of the wings consisted of four active semiconductor strain gages forming a complete bridge. Prior to the wind-on investigation of the models, each of the models was oscillated at

known frequencies by means of an audio speaker located under the wing. The models were oscillated through a range of frequencies from 0 to 400 Hz to determine the bending characteristics of the wing and to ensure that the gages were sensitive to oscillation at the fundamental bending frequencies. The equipment used in this static survey, in addition to the audio speaker, included a proximity pickup placed close to each wing tip hooked up to a dual beam oscilloscope. As the frequency of the speaker was increased through the known frequency range, the phase relationship and the amplitude of the pickups were observed on the oscilloscope screen. Frequencies were recorded as fundamental frequencies where the oscilloscope signal revealed a relative maximum. Subsequent spectral analysis of the root mean square (rms) wind tunnel data confirmed the fundamental frequencies determined from the static tests.

The buffet strain gage output was recorded on FM magnetic tape for a period of approximately 60 seconds per data point. For each 60-second period, data were digitized onto magnetic tape and then processed on a CDC 6700 computer to calculate the rms value of the wing-root bending moment.

ANALYSIS OF THE 25-DEGREE WING AERODYNAMICS

Common to all the canard configurations is the continuing increase in lift coefficient beyond the point at which the wing alone configuration stalls. As a consequence of the delayed stall, the drag at higher lift coefficients for the configurations with canards is lower than that for configurations without canards. At lower lift coefficients the drag values are about equal. Furthermore, although the longitudinal stability decreases with the addition of canards, the C_L versus C_M curve remains fairly linear to high values of lift coefficients as opposed to a typical sharp break in longitudinal stability at wing stall without canards. Figure 5 shows these trends for a typical set of configurations at a Mach number of 0.8.

DRAG

The canard placed ahead of and at a negative angle of deflection relative to the wing can act to prevent flow separation on the wing. At the same time, to minimize its pressure drag, the negative deflection of the

canard should be kept to a minimum. Thus, drag tends to be lowest over the Mach number range for canard deflections between 0- and -5-degrees and increases for deflections in either direction beyond this range; see Figure 6.

At low values of lift coefficient there is no significant change in drag with canard position; however, at higher values of lift coefficient, a canard position ahead of and above the wing (P_3) yields the lowest drag values (as shown in Figure 7).

Over the transonic Mach number range, as long as the lift coefficient is below stall, there is a slight penalty in drag for carrying the canard as compared to the wing-body combination. However, because of the capability of the canards to alleviate stall, significantly lower drag values are experienced for the configurations with canards in comparison to those with wing alone when the wing has stalled; see Figure 8.

LIFT

While the lift gains are not significant for the configurations with canards at low angles of attack, lift gains are sizable for configurations with canards at higher angles of attack. This effect for the C_{D_o} canard over the Mach number range is shown in Figure 9. It can also be observed from this figure that as the canard deflection increases, so does the lift coefficient.

A canard position ahead of and above the wing yields the greatest lift benefit; see Figure 10. In comparing canard-on with canard-off configurations (Figure 11), significant lift gains were achieved at an angle of attack of 20-degrees for the canard-on configurations.

LIFT-TO-DRAG RATIOS

The maximum lift-to-drag ratio of an aircraft is used to represent its cruise efficiency. Canard deflection angle, as seen in Figure 12, has a significant effect on maximum L/D ratio. In this figure it is observed

that a canard deflection of -5-degrees results in the best maximum L/D with a variation in deflection angle in either direction being detrimental. Canard position does not have a major effect on maximum L/D within the range of the experimental data presented in Figure 13.

A penalty in maximum L/D (Figure 14) must be paid for the addition of canards; however, with proper tuning of the canard deflection angle, this penalty can be kept to a minimum. Furthermore, Figure 15 shows that at lift coefficients beyond wing/body stall, L/D values for configurations with canards are substantially better than the values for configurations without canards.

BUFFET DATA

Buffet data in the form of rms values of the wing bending moment, as well as lift coefficients for buffet onset as determined from these rms values and axial forces, are presented in Figures 16 through 19. Unfortunately, no clear trends are discernable for the 25-degree wing. The canards do not appear to be beneficial in alleviating buffet intensity. The explanation for this may be that the 25-degree sweep of this wing is too low to make it a good transonic airfoil. Consequently, the flow over the wing begins to separate and buffet occurs well before the downwash from the canards is able to act to prevent flow separation. This conclusion is supported by the data presented in Reference 3 where it is observed that there is a sizable increase in buffet intensity as the wing sweep is reduced from 45- to 35- to 25-degrees.

ANALYSIS OF THE 50-DEGREE WING AERODYNAMICS

A typical data set comparing configurations with and without canards is presented in Figure 20 for a Mach number of 0.80. Common to other configurations with canards is the gain in lift coefficient at higher angles of attack, the decrease in drag coefficient and the increase in lift-to-drag ratios at higher values of lift coefficient, and the fairly linear static longitudinal stability curve.

DRAG

Canard deflection angles between 0- and -5-degrees produce minimum drag over the Mach number and C_L range investigated; see Figure 21. At lift coefficients close to zero, zero-degree canard deflections result in the lowest drag. With the canard deflected at -5-degrees, both the wing and the canard are producing some small value of lift, although the overall lift coefficient is near zero. Therefore, a small amount of induced drag is present at the -5-degree deflection. At higher lift coefficients a canard deflection angle of -5-degrees is more desirable. Canard planform and position locations within the scope of the data presented in Figures 22 and 23 appear to have little significant effect on drag.

The effect on drag of the canard-on compared with the canard-off configuration with and without a horizontal tail at various lift coefficients is presented in Figure 24. At the low values of C_L, the lowest drag is obtained for the wing-body combination. However, even at these low values of C_L, the wing/canard configuration has a lower value of drag than the wing-tail configuration. At the high value of C_L, the drag savings of the canard-on configuration with and without a horizontal tail is very significant.

The decrease in drag with increase in Mach number at the high values of C_L, as shown in both Figures 8 and 24, requires some explanation. First, referring to the C_L versus C_D and the C_L versus α curves presented in References 1 and 2, the decrease in drag with an increase in Mach number begins to occur at a C_L close to where the C_L versus α curve indicates the onset of a stall. It therefore is a valid conclusion that as the Mach number increases, the stall is either reduced in severity or delayed altogether. This effect is perhaps as described in Reference 4 (page 643). As the Mach number increases, the shock wave on the upper surface of the airfoil moves back. As the shock moves back, so does the point of transition and/or the point of flow separation because the pressure gradient is usually favorable as far back as the shock wave. Thus, there is a reduction of drag due to the more rearward shock position which outweighs

the increase in drag due to the loss of energy at the shock wave as the shock strength increases with Mach number.

One further item in Figures 8 and 24 requires explanation. In these figures, the drag decreases with increase in Mach number for all configurations except the canard-on configurations for the 50-degree wing. The explanation for this might be that the canard has already successfully delayed the stall of the wing. Therefore, the rearward movement of the shock does not serve to alleviate or delay the stall, but rather the increased strength of the shock and the consequent losses simply increase the drag for these configurations.

LIFT

As for the 25-degree sweep wing, the gains in C_L for the 50-degree wing with the addition of canards become significant at higher angles of attack. Lift coefficient tends to increase with canard deflection angle as shown in Figure 25.

Prior to stall the highest values of C_L for the 50-degree wing with the addition of canards become significant at higher angles of attack. Lift coefficient tends to increase with canard deflection angle as shown in Figure 25.

Prior to stall the highest values of C_L are obtained for the lowest sweep canard as shown in Figure 26; however, the lowest sweep canard also tends to stall earliest. Thus, while the 25-degree sweep canard in Figure 26 shows the highest values of lift coefficient and the 60-degree sweep canard shows the lowest values, the 60-degree sweep canard stalls later than the 25-degree sweep canard.

The effect of canard position variation on lift coefficient, within the range of positions presented in Figure 27, shows no significant effect. At an angle of attack of 20-degrees, there is a significant advantage of the canard as compared to the horizontal tail configuration (presented in Figure 28). The latter figure shows that gains on the order of 20-percent

in untrimmed lift coefficient over the Mach number range tested are available with the addition of properly placed and properly deflected canards.

LIFT-TO-DRAG RATIOS

Using maximum L/D as a measure of overall performance, Figure 29 shows that, overall, a canard deflection angle of -5-degrees is best with significant movement from this canard deflection angle having a drastic effect on maximum L/D. Variations in canard planform (presented in Figure 30) indicate that a 45-degree sweep delta canard yields the best overall performance, while canard position (as shown in Figure 31) has little effect on maximum L/D.

While the best maximum L/D performance is attained by the wing/fuselage combination (as shown in Figure 32), the configuration with the canards in addition to the tail shows a consistent gain over the tail alone configuration for the entire Mach number range evaluated. Furthermore, at higher lift coefficients, the addition of canards yields a significant improvement in L/D even in comparison to the wing/fuselage combination.

BUFFET DATA

Buffet intensity does not appear to be highly sensitive to canard planform (as shown in Figure 33). A slight reduction in overall buffet intensity is obtainable from the 45-degree delta canard. Vertical position variation in proximity to the wing does not significantly effect buffet intensity; however, as Figure 34 shows, movement of the canard forward of the wing does significantly increase the buffet intensity level. Furthermore, at low values of lift coefficient only a slight decrease in buffet intensity is obtained in comparing configurations with a horizontal tail to those with canards; see Figure 35. However, a comparison of these configurations at higher lift coefficients shows a significant decrease in buffet intensity.

Trends in buffet onset lift coefficient parallel those of buffet intensity, as shown in Figures 36 through 38. The 45-degree delta canard at

a position forward of and slightly above the wing yields the highest buffet onset lift coefficient. In addition, buffet onset lift coefficient is significantly higher for the configuration with canards as compared to a configuration with horizontal tails.

COMPARISON OF THE 25- AND 50-DEGREE WINGS

The 25-degree sweep wing yields lower drag and better maximum L/D performance below its drag divergence Mach number of 0.85 when compared to the 50-degree sweep wing (see Figures 39 and 40). However, the 50-degree wing yields higher lift values at high angles of attack and does not reach a drag divergence Mach number in the range evaluated.

A comparison of the two wing sweeps with the addition of identical canards, as shown in Figures 41 and 42, reveals the same trends as the wings themselves. That is, below drag divergence and at low angles of attack the 25-degree sweep wing is superior; while above drag divergence and at higher angles of attack the 50-degree wing is superior.

CONCLUSIONS

The following conclusions are drawn from the analysis presented in this report:

1. Of the canard planforms and positions evaluated, the best overall performance can be obtained from a 45-degree delta canard deflected between 0- and -5-degrees and positioned slightly above and forward of the wing with slight overlap.

2. Canard configurations show the most significant gains in lift and drag over a standard horizontal tail configuration at high angles of attack.

3. Buffet alleviation by means of canards is insignificant for low wing sweep. However, for higher wing sweep and at high lift coefficient, canards can delay buffet onset and alleviate buffet intensity.

4. The 25-degree wing with canards is a desirable option for an attack/bomber-type aircraft designed to fly long cruise missions at Mach numbers less than 0.85. The 50-degree wing, in conjunction with canards, would do well on an aircraft designed to perform as a highly maneuverable fighter.

REFERENCES

1. Ottensoser, J., "Test Data on the Transonic Aerodynamic Characteristics of Close-Coupled Canards with Varying Position and Deflection Relative to a 25-Degree Swept Wing," NSRDC Test Report AL-87, AD-891-816 (Jan 1972).

2. Ottensoser, J., "Wind Tunnel Data on the Transonic Aerodynamic Characteristics of Close-Coupled Canards with Varying Planform, Position and Deflection Relative to a 50-Degree Swept Wing," NSRDC Test Report AL-88, AD-900-294 (May 1972).

3. Ray, E.J. and R.T. Taylor, "Buffet and State Aerodynamic Characteristics of a Systematic Series of Wings Determined from a Subsonic Wind Tunnel Study," NASA TN D-5805 (Jun 1970).

4. "Modern Developments in Fluid Dynamics: High Speed Flow," Vol. II, edited by L. Howarth, Oxford-Clarendon Press, London (1953).

TABLE 1 - GEOMETRIC CHARACTERISTICS OF THE WINGS

	50-Degree Sweep	25-Degree Sweep
Projected Area, square inches	304	295
Span, inches	35.50	42.00
Chord, inches		
Root (centerline)	15.38	12.20
Tip	1.90	1.90
Mean Aerodynamic Chord, inches		
Length	10.30	8.30
Spanwise Location from Body Centerline	6.70	7.90
Aspect Ratio	4.15	6.00
Taper Ratio	0.12	0.16
Sweepback Angle, degrees		
Leading Edge	50.0	25.0
Quarter Chord	45.5	20.0
Trailing Edge	23.5	-1.5
Incidence Angle, degrees	0	0
Dihedral Angle, degrees	0	0
Twist Angle, degrees	0	0

TABLE 2 - CANARD GEOMETRY				
	Canard			
	0	1	2	3
Airfoil Section (NACA)	64A008	64A006	64A008	64A008
Exposed Area, square inches	39.8	39.8	47.2	49.3
Projected Area, square inches	76.0	89.5	76.0	76.0
Exposed Semispan, inches	5.74	4.79	7.60	7.60
Total Span, inches	16.28	14.38	20.00	20.00
Chord, inches				
Root (centerline)	8.73	12.45	6.70	6.12
Root (exposed)	6.33	8.30	5.31	5.00
Tip	0.59	0	0.90	1.48
Aspect Ratio	3.50	2.21	5.26	5.26
Taper Ratio	0.70	0	0.13	0.24
Sweepback Angle, degrees				
Leading Edge	45.0	60.0	45.0	25.0
Trailing Edge	0	0	22.8	0
Dihedral Angle, degrees	0	0	0	0

Figure 1 - Aircraft Model Geometry

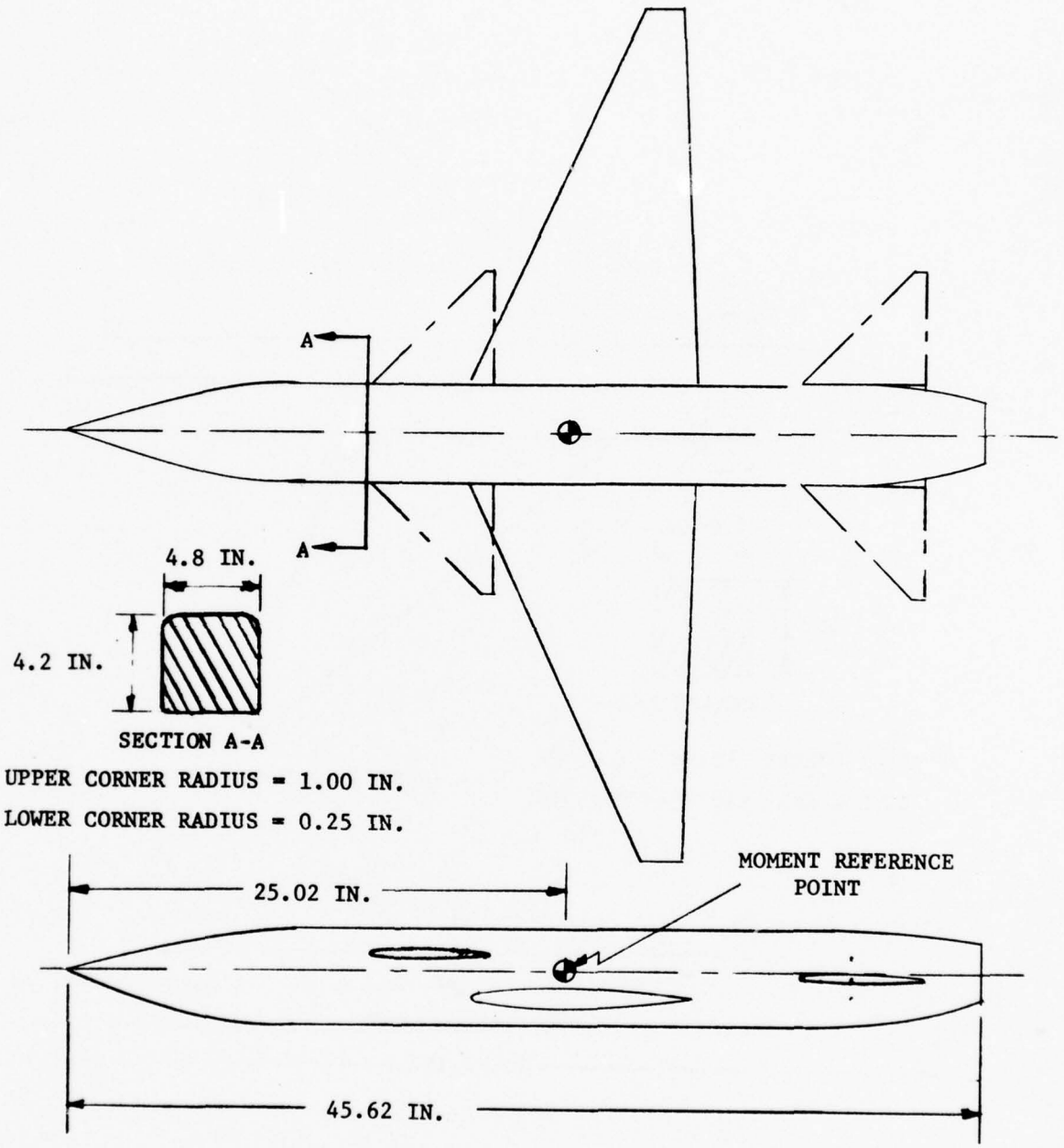

Figure 1a - 25-Degree Leading Edge Sweep Wing

Figure 1 (Continued)

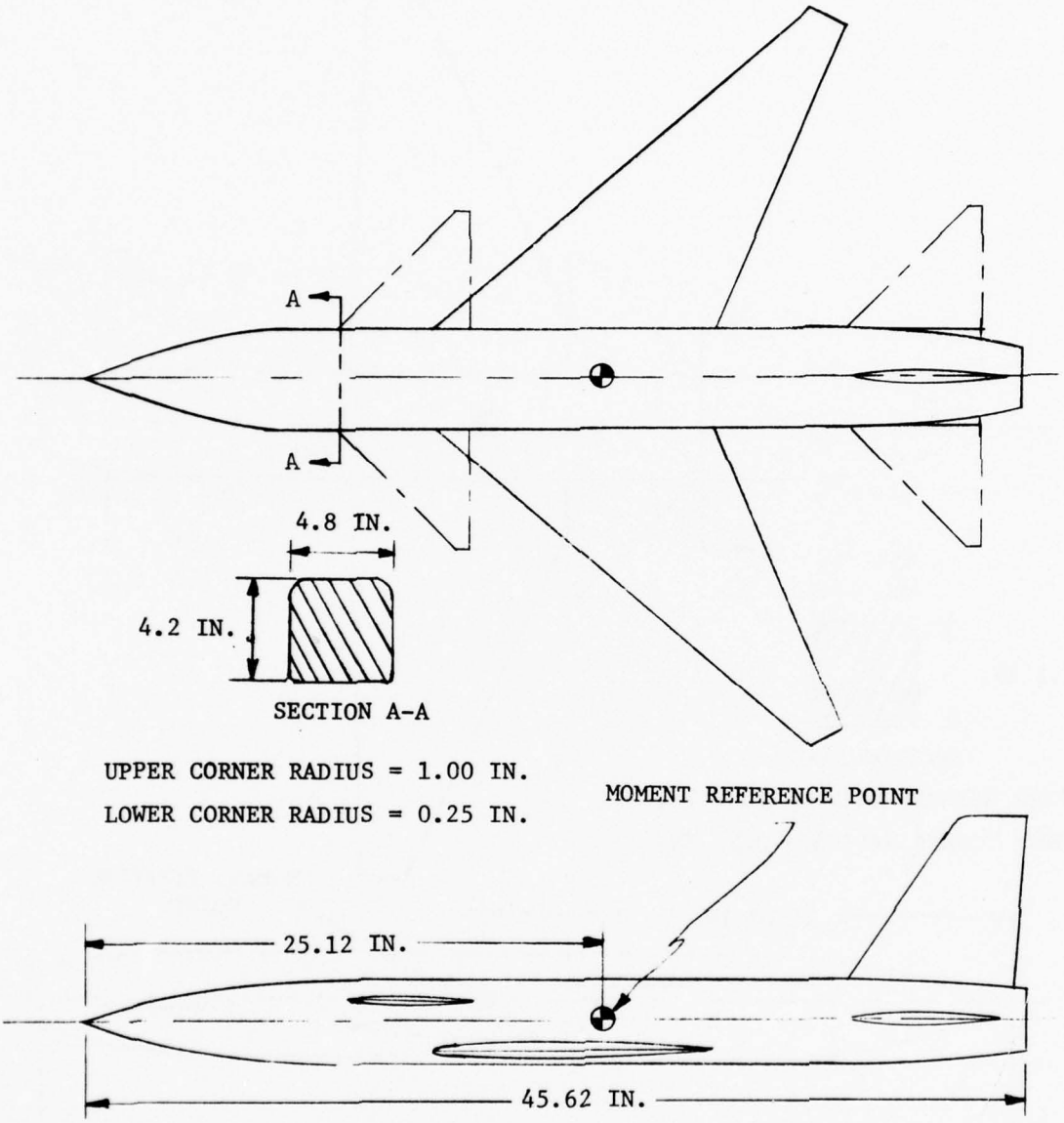

Figure 1b - 50-Degree Leading Edge Sweep Wing

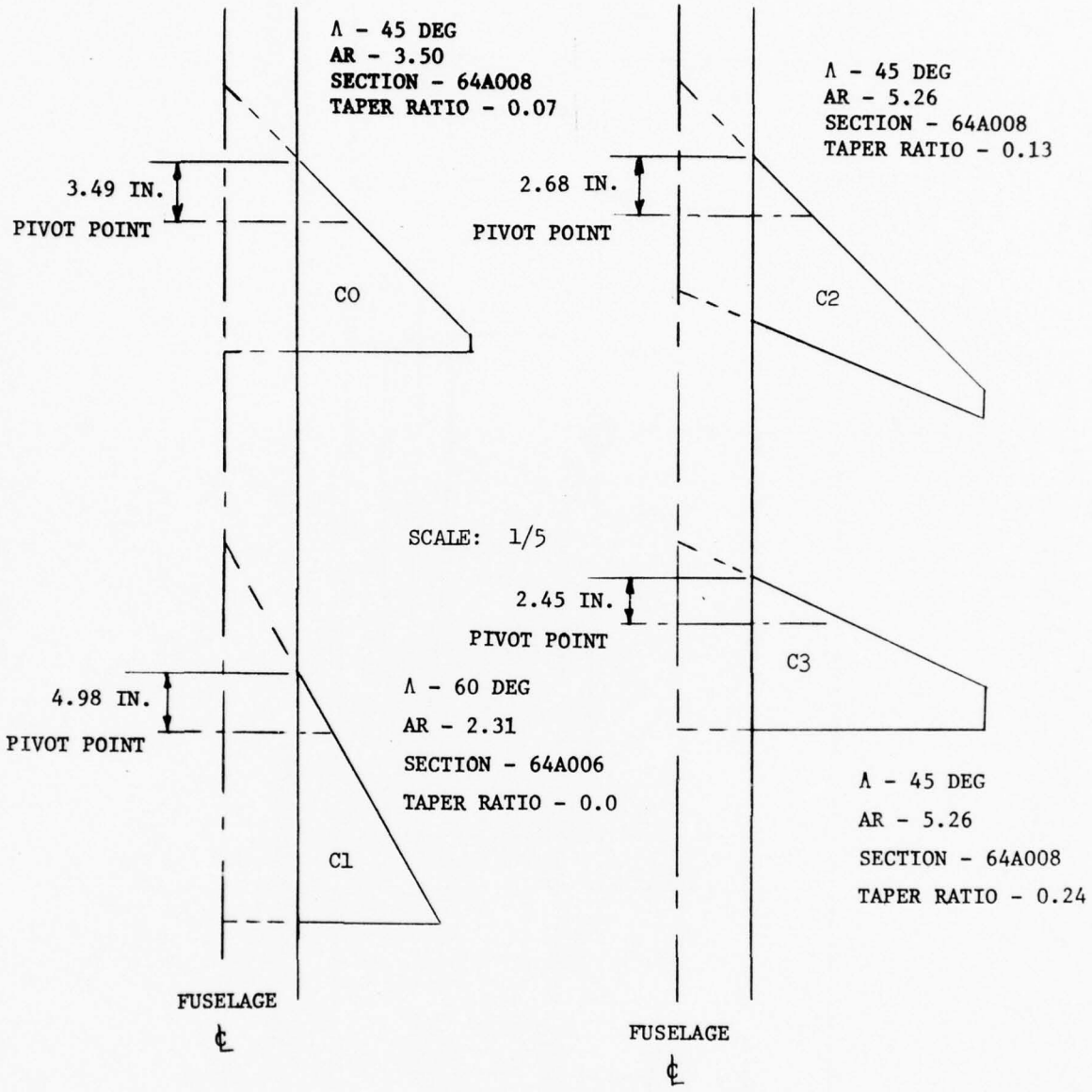

Figure 2 - Canard Geometry

Figure 3 - Canard and Horizontal Tail Pilot Locations
(All dimensions are in inches)

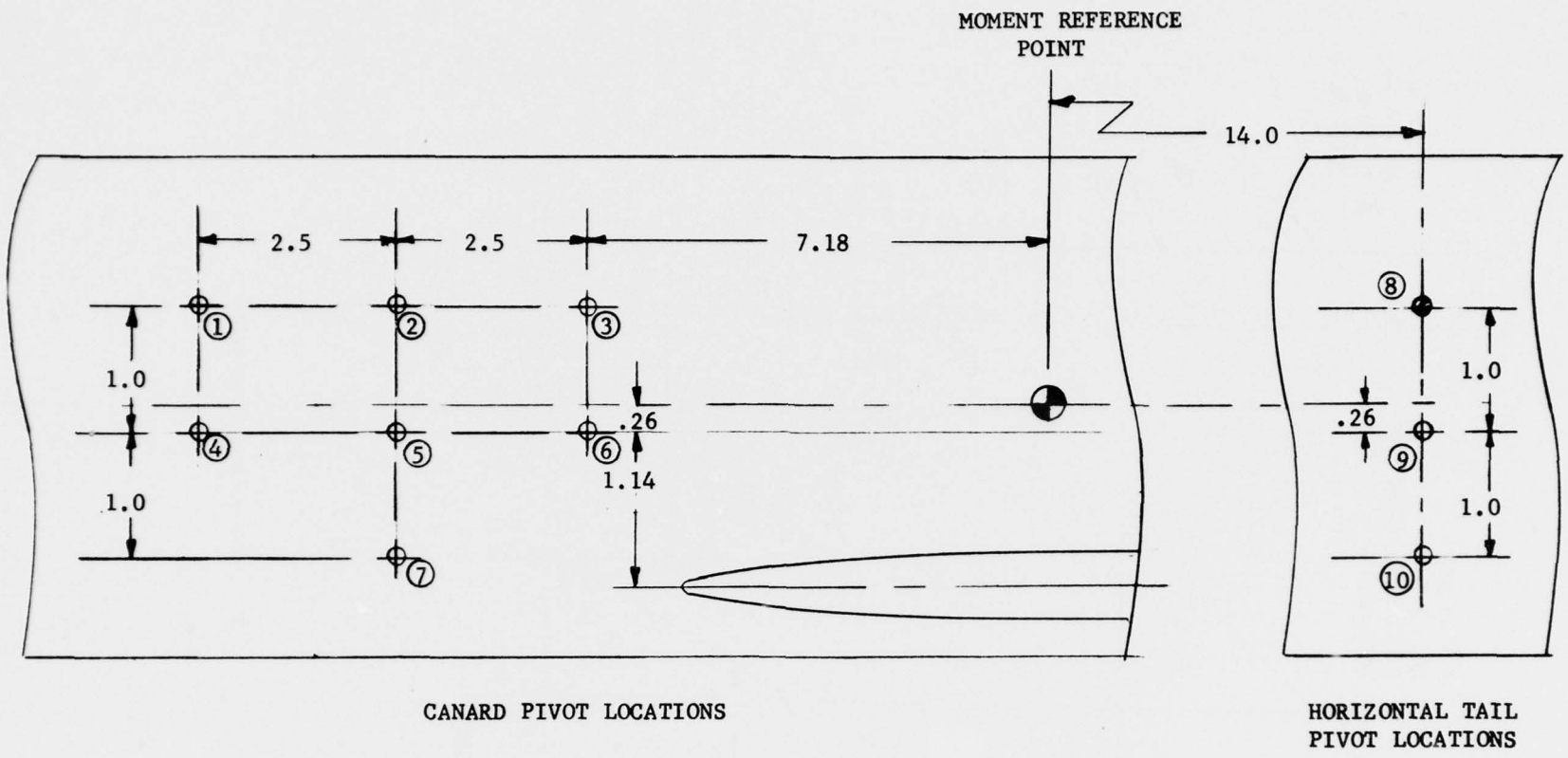

Figure 3a - Locations Relative to the 25-Degree Sweep Wing

Figure 3 (Continued)

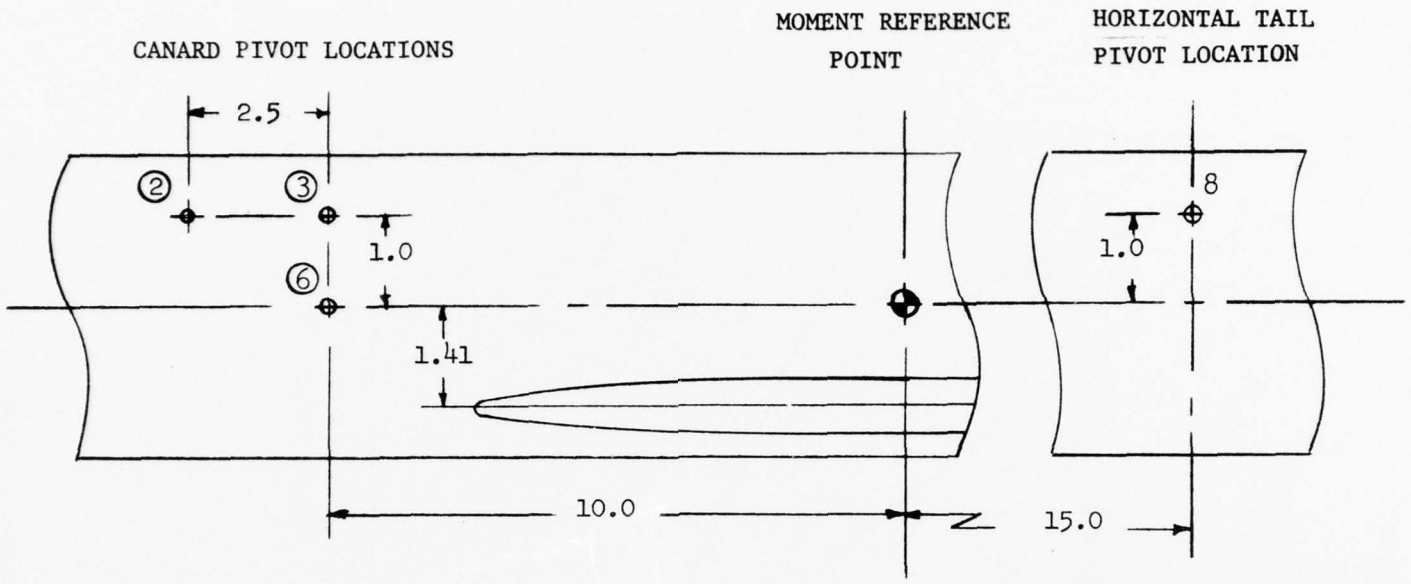

Figure 3b - Locations Relative to the 50-Degree Sweep Wing

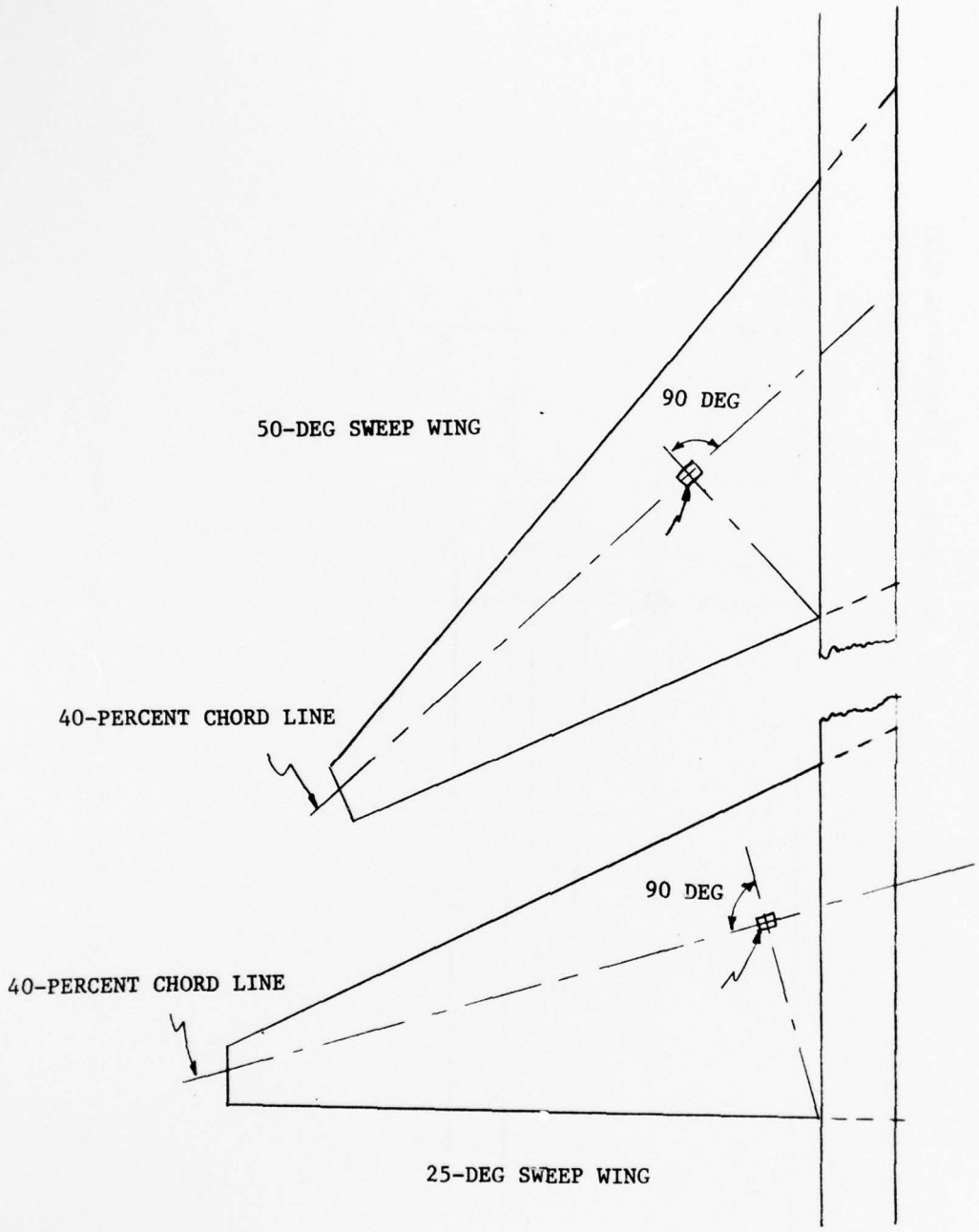

Figure 4 - Location of Wing-Root Bending Gages

Figure 5 - Comparison of Configurations with and without Canards for the 25-Degree Sweep Wing

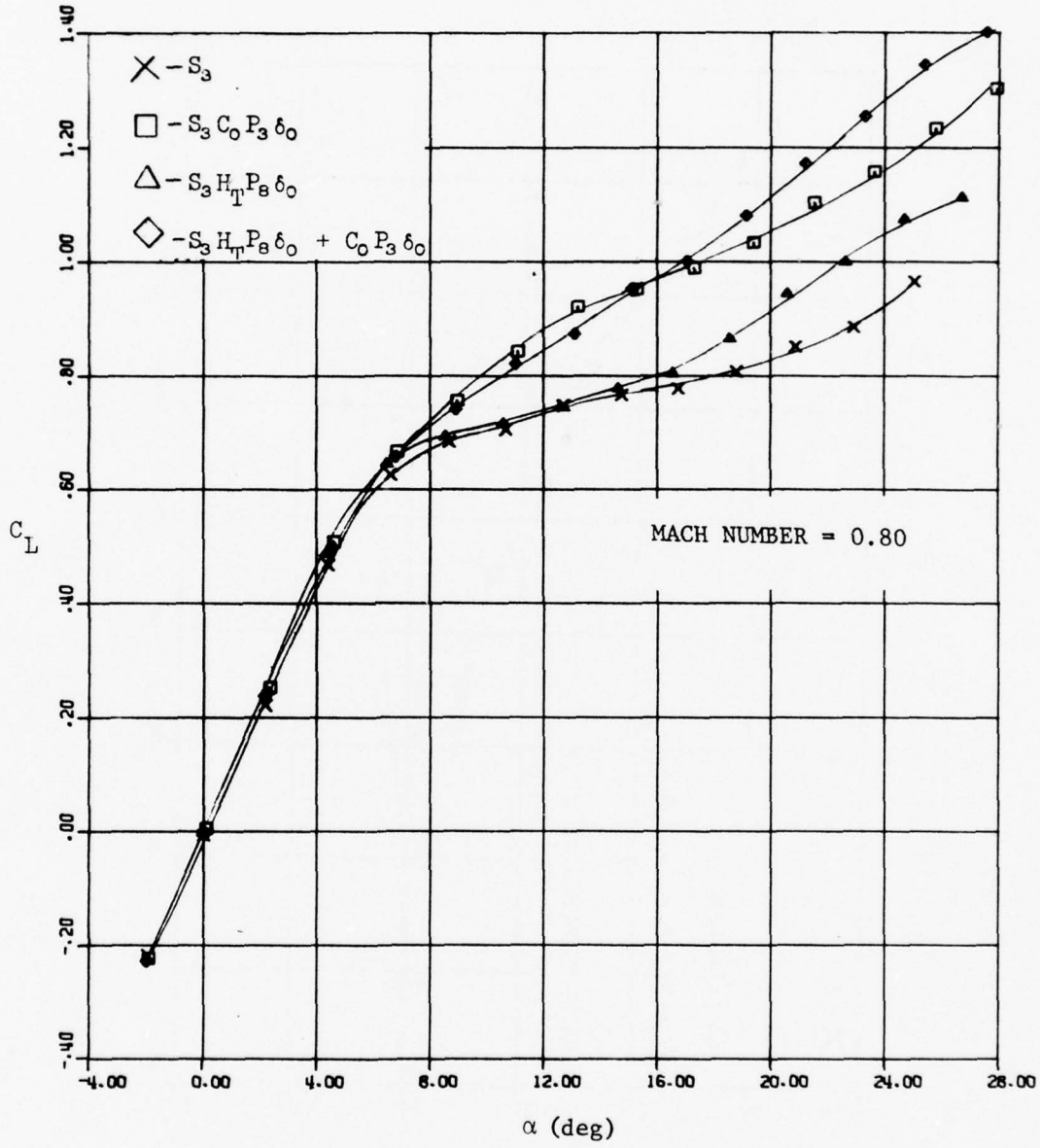

Figure 5a - C_L versus α

Figure 5 (Continued)

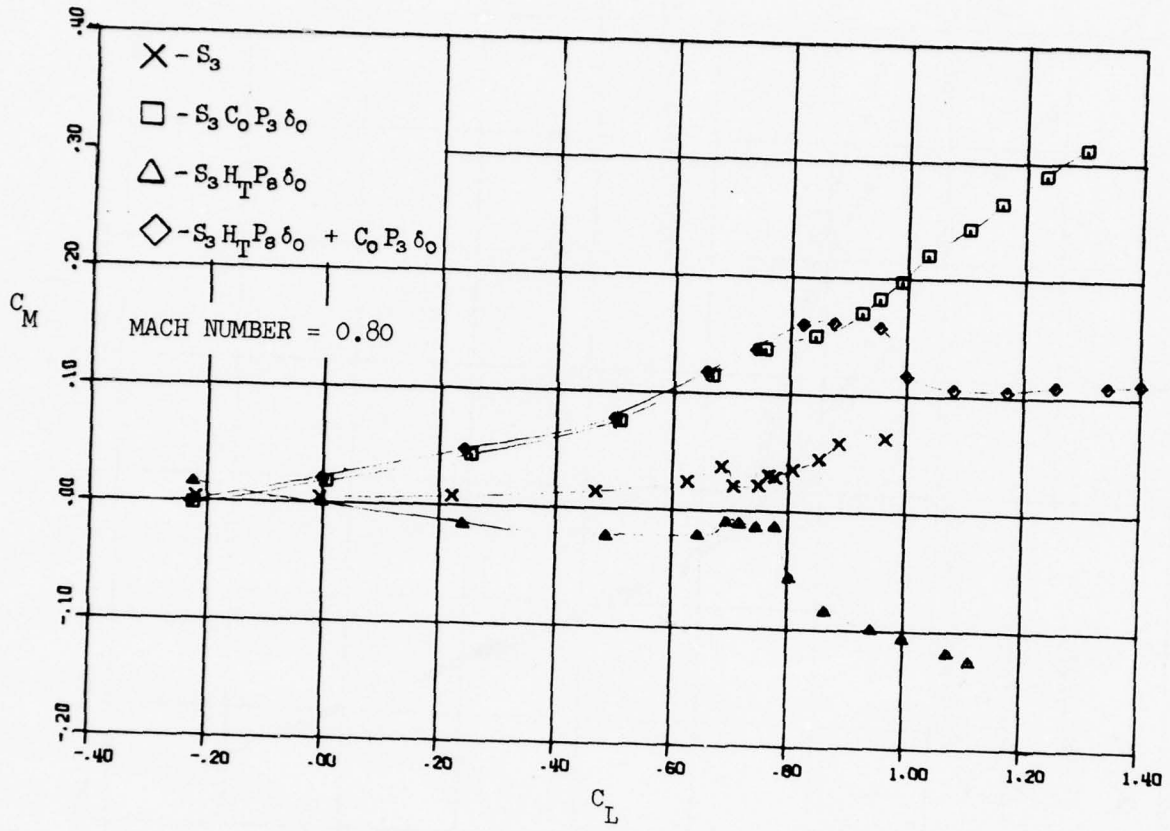

Figure 5b - C_M versus C_L

Figure 5 (Continued)

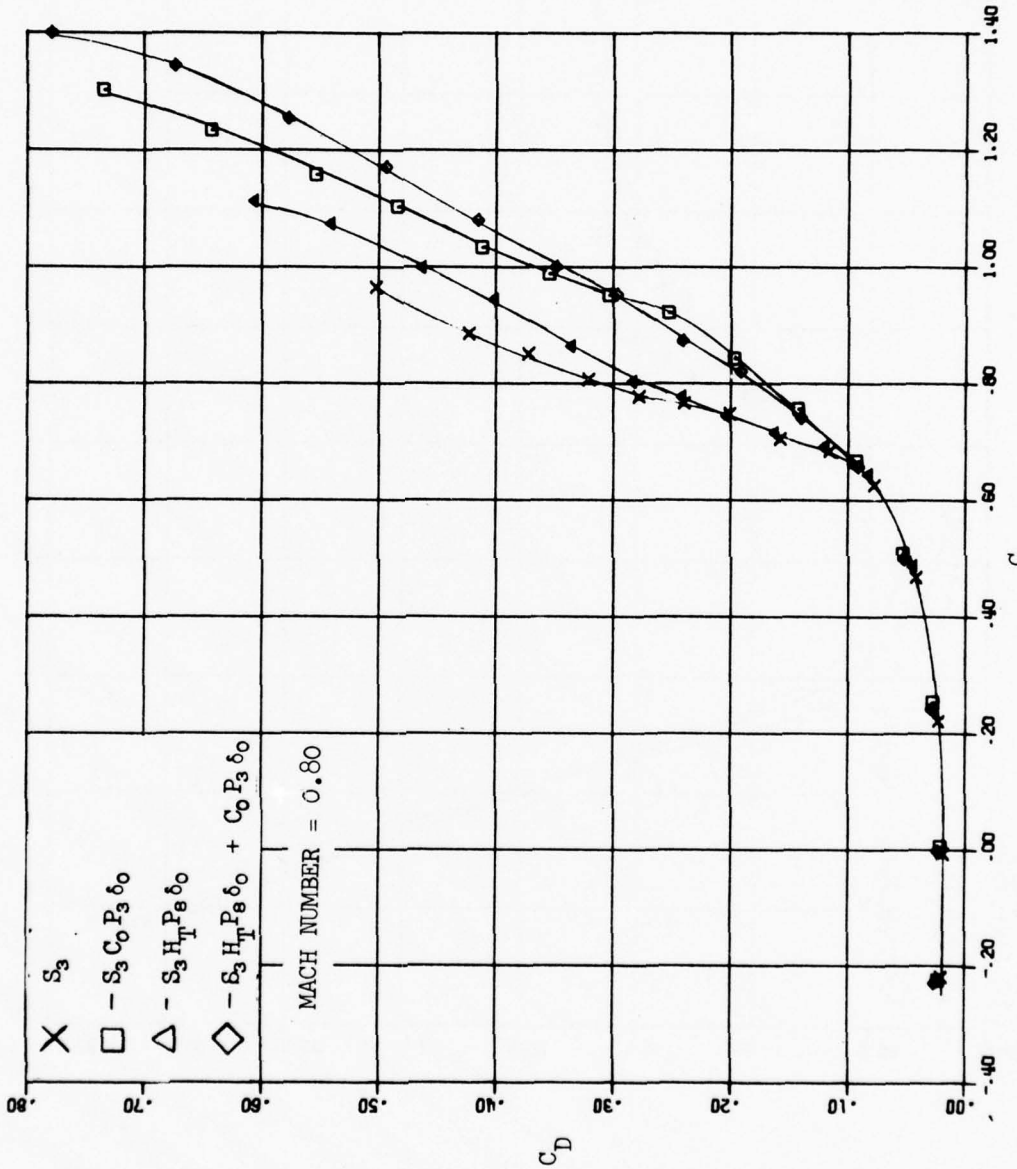

Figure 5c - C_D versus C_L

Figure 5 (Continued)

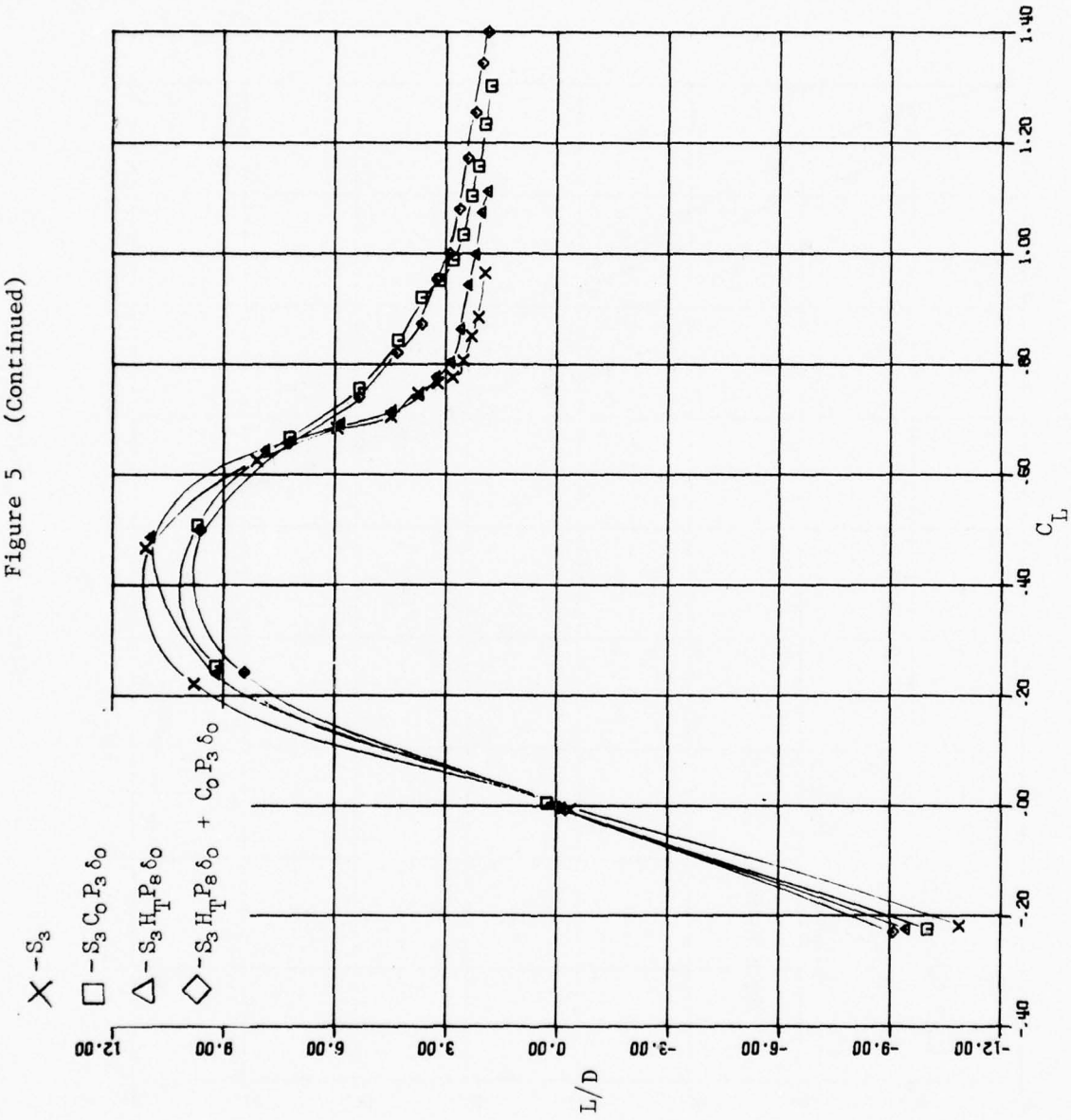

Figure 5d - L/D versus C_L

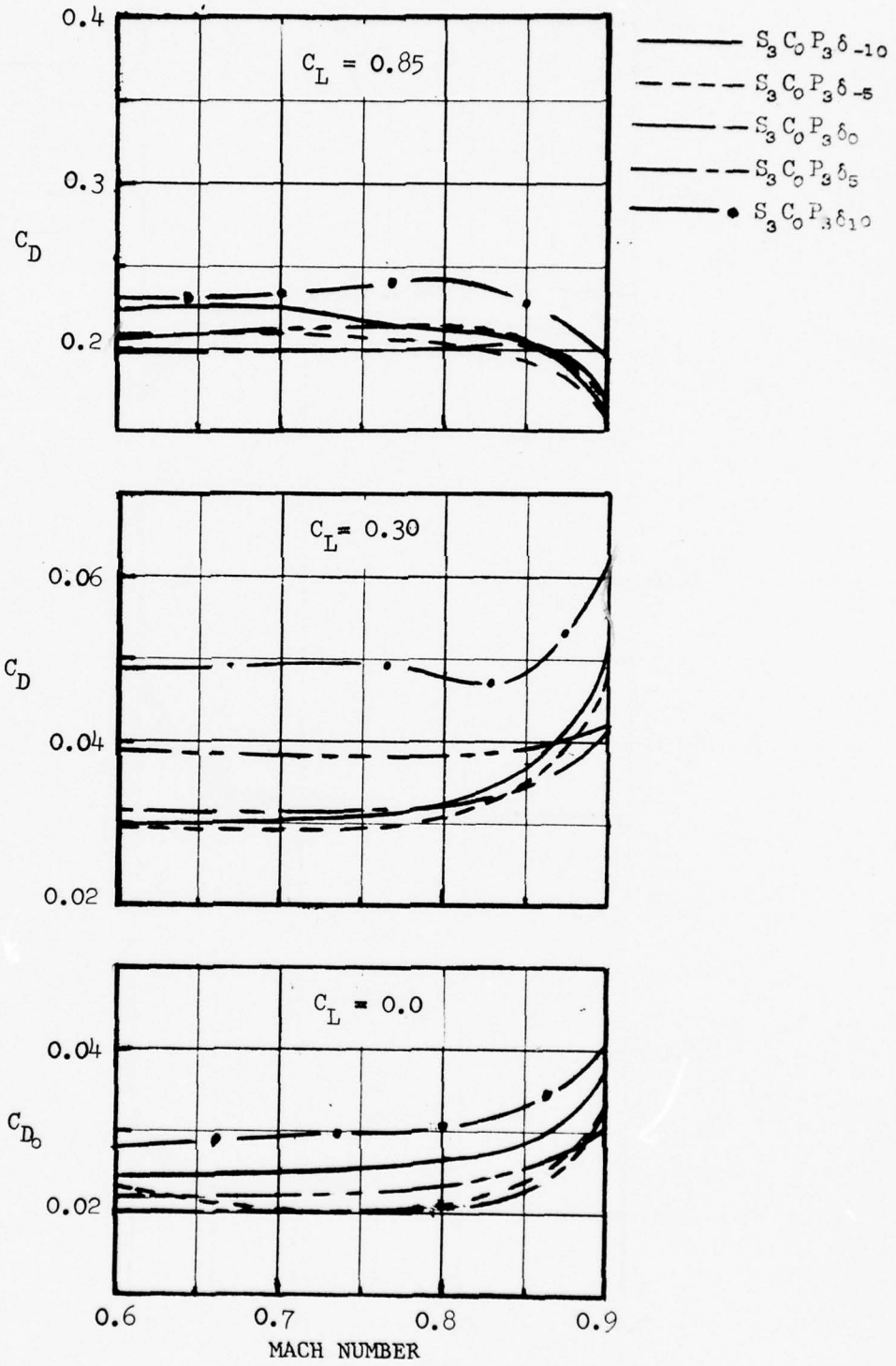

Figure 6 - Effect of Canard Deflection Angle on Drag for the 25-Degree Sweep Wing

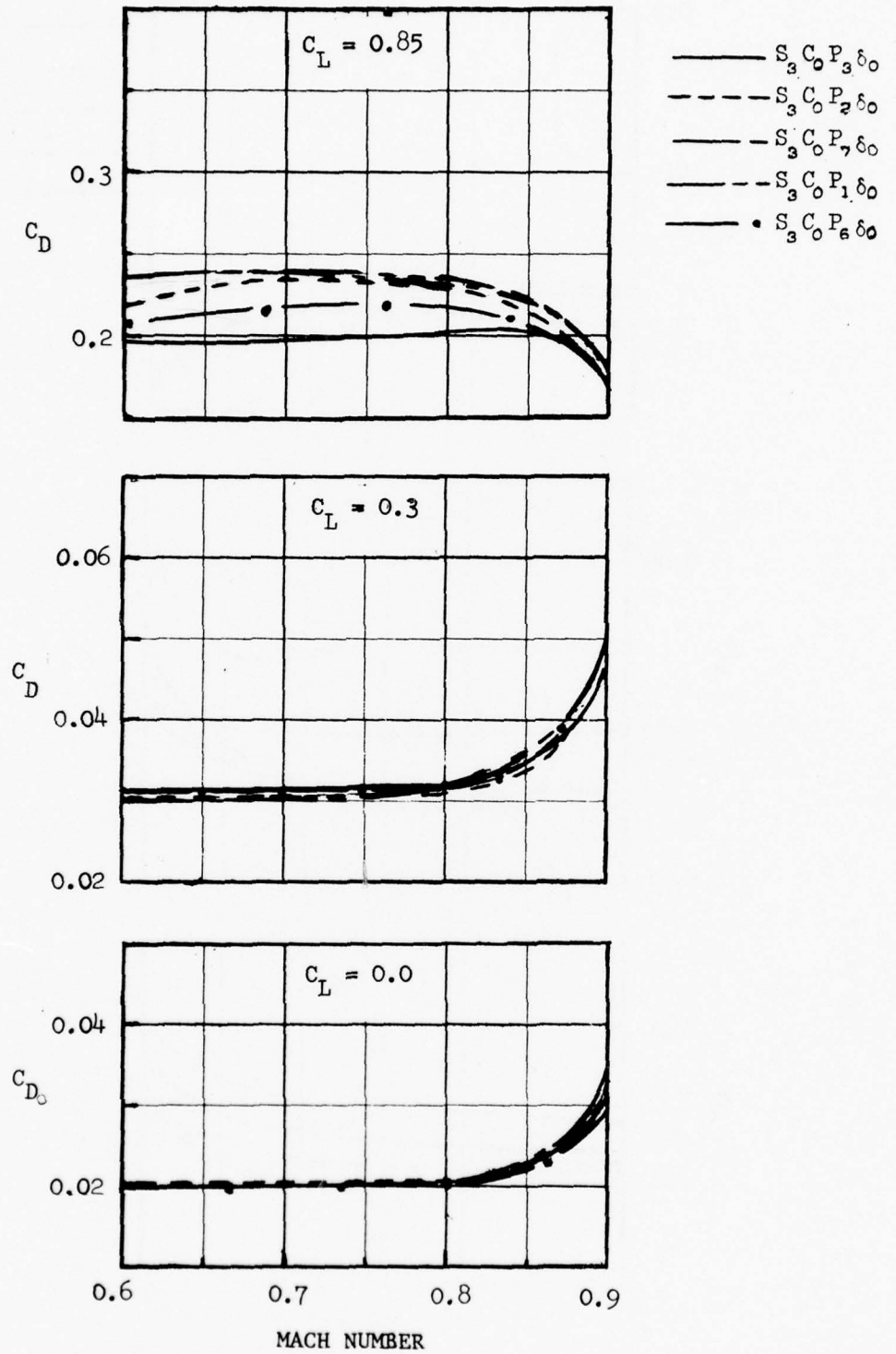

Figure 7 - Effect of Canard Position on Drag for the 25-Degree Sweep Wing

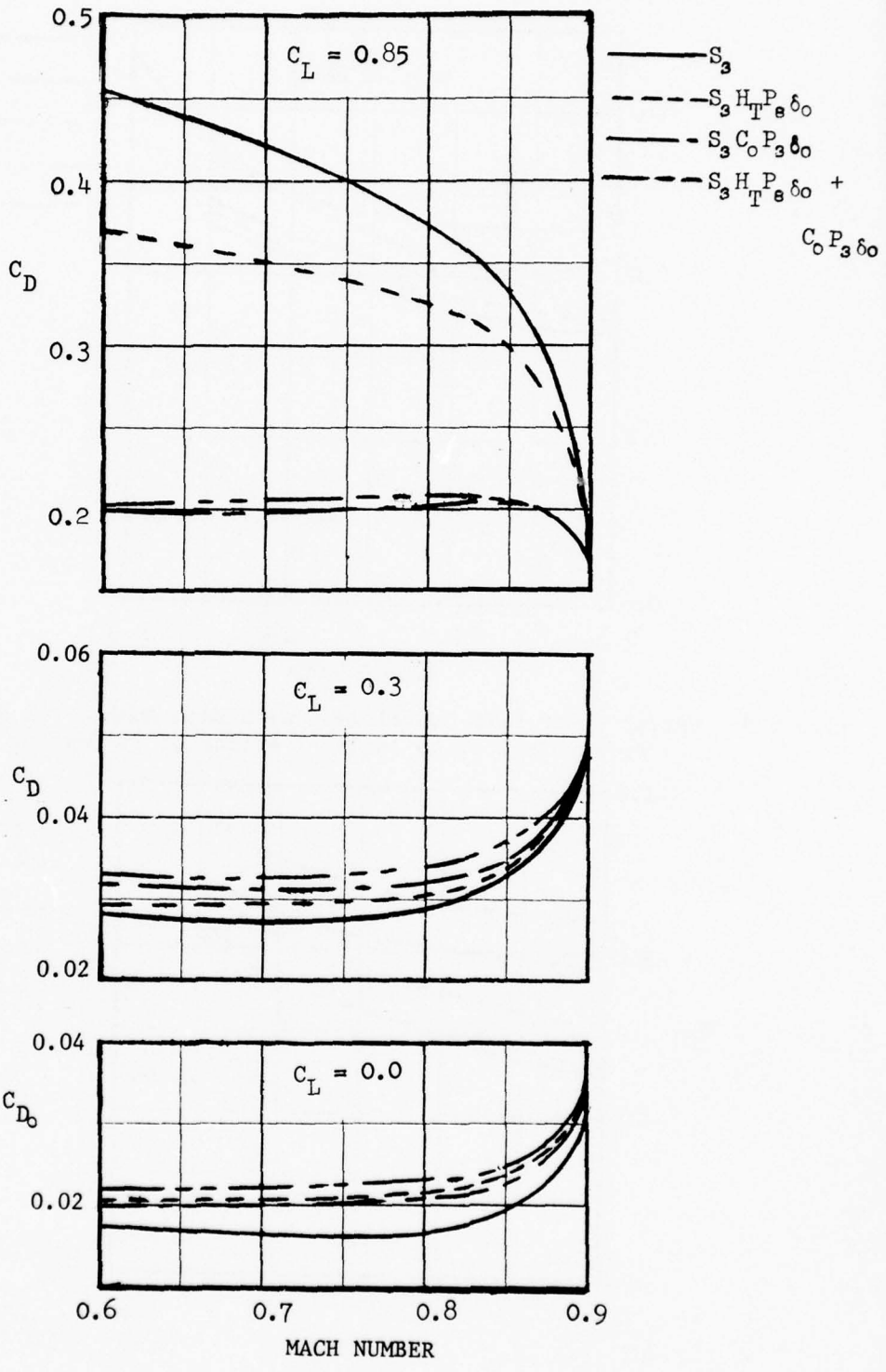

Figure 8 - Comparison of Drag Coefficients for Configuration with and without Canards for the 25-Degree Sweep Wing

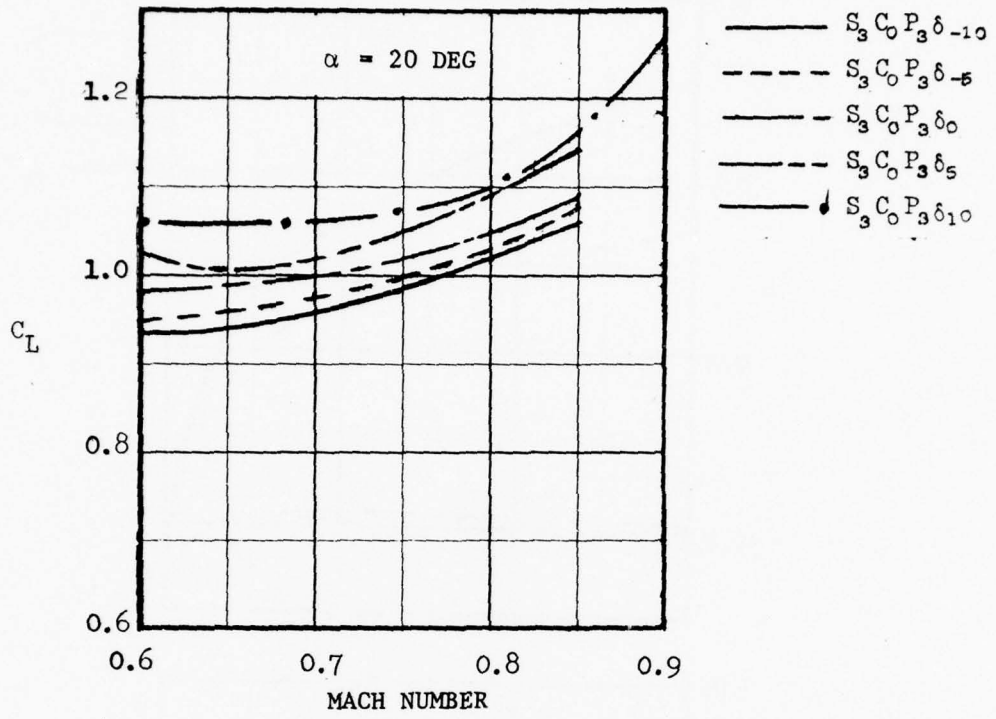

Figure 9 - Variation of Lift Coefficient with Mach Number for Several Canard Deflections at an Angle of Attack of 20 Degrees

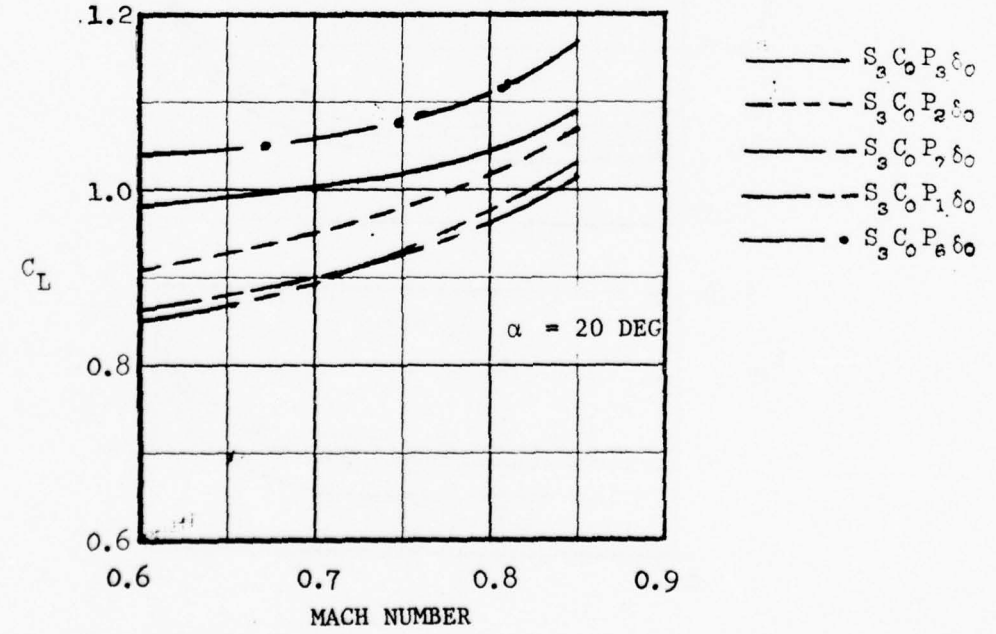

Figure 10 - Variation of Lift Coefficient with Mach Number for Several Canard Positions at an Angle of Attack of 20 Degrees

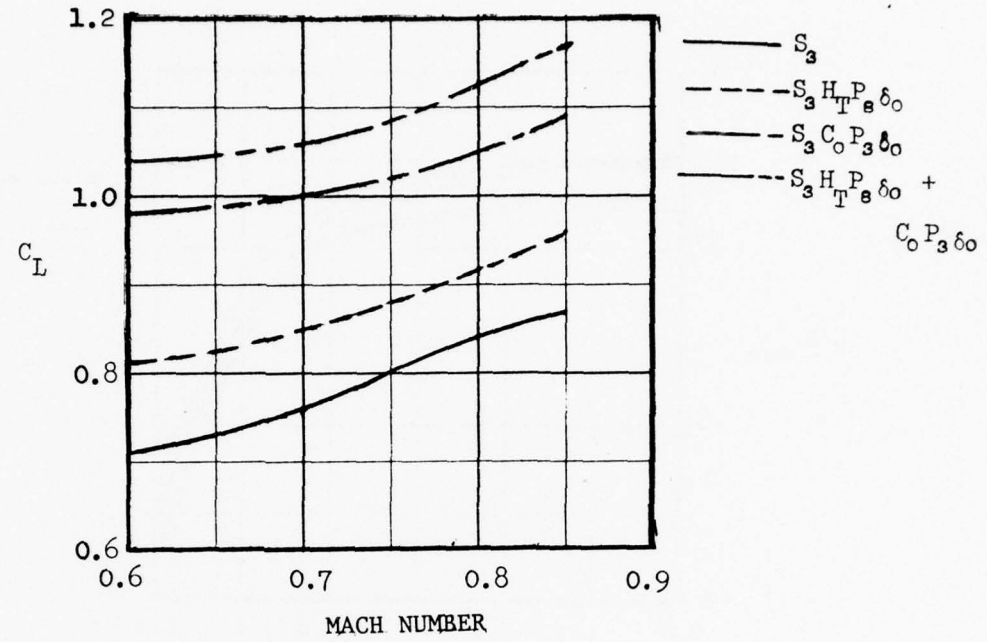

Figure 11 - Variation of Lift Coefficients with Mach Number at an Angle of Attack of 20 Degrees for Configurations with and without Canards

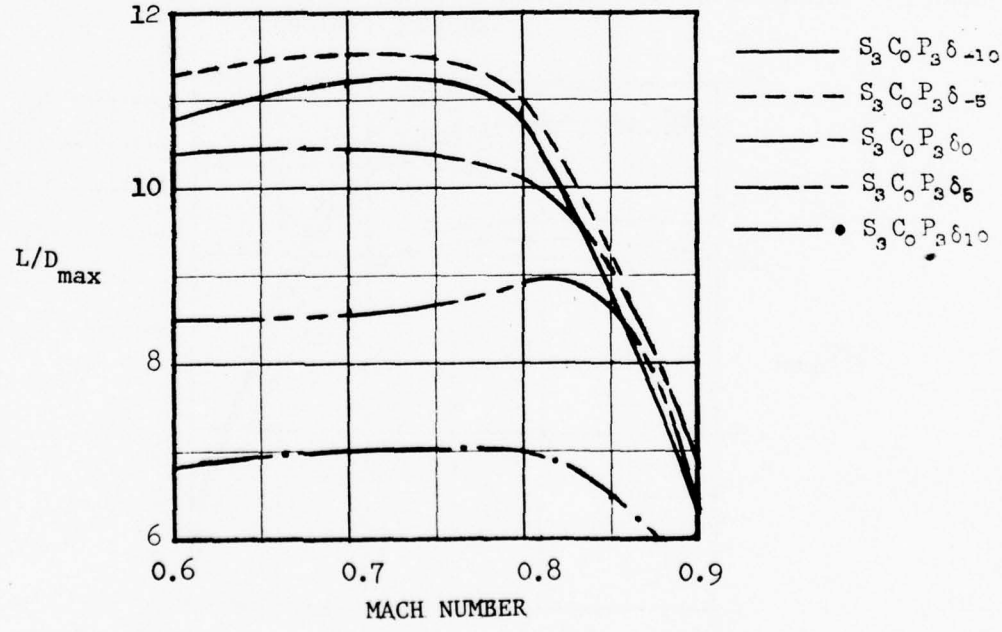

Figure 12 - Variation of Maximum Lift-to-Drag Ratio with Mach Number for Several Canard Deflection Angles

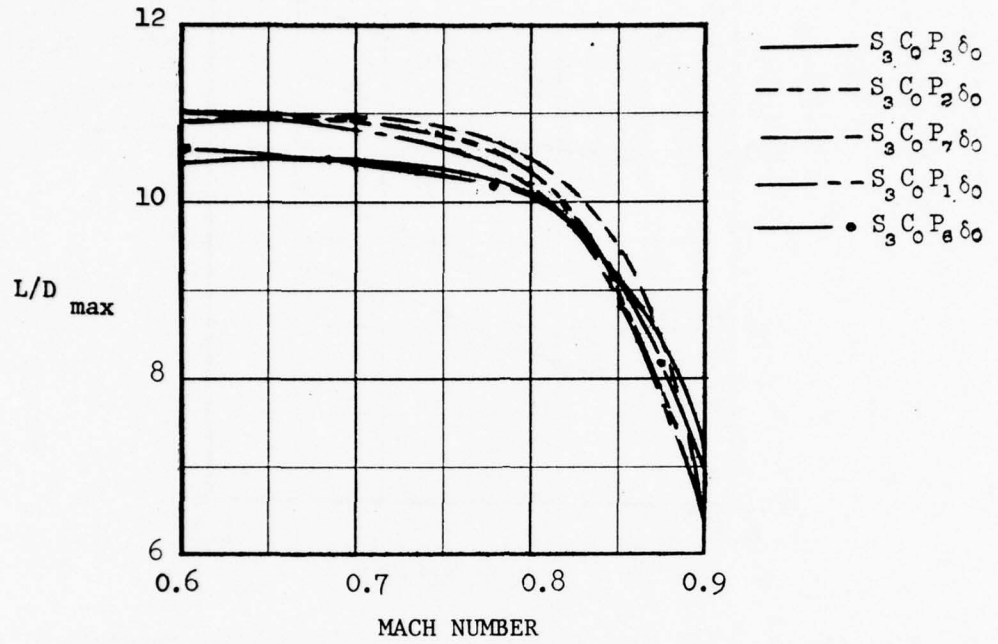

Figure 13 - Variation of Maximum Lift-to-Drag Ratio with Mach Number for Several Canard Positions

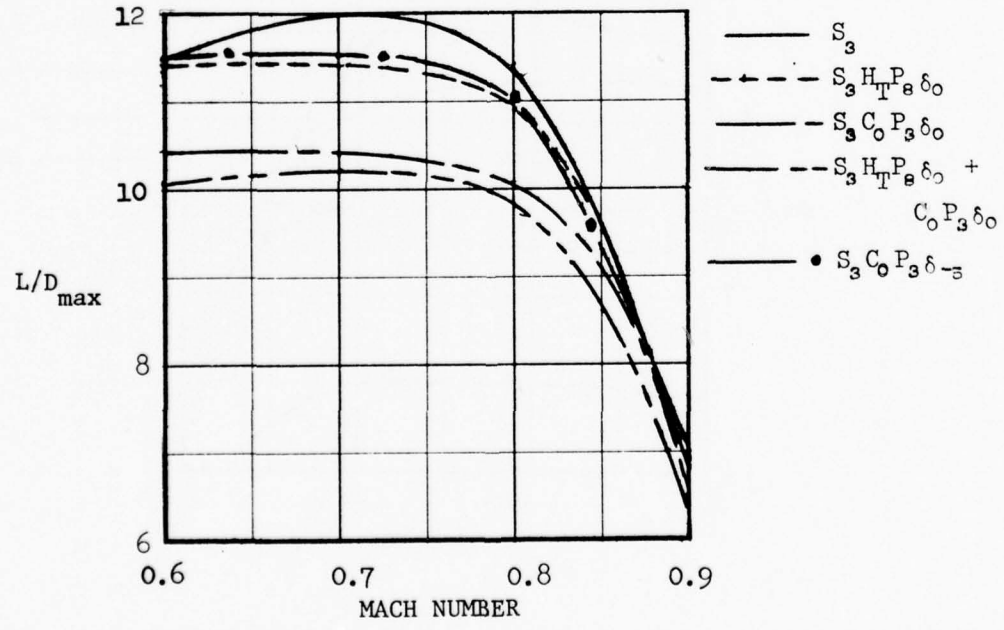

Figure 14 - Variation of Maximum Lift-to-Drag Ratios with Mach Number for Configurations with and without Canards

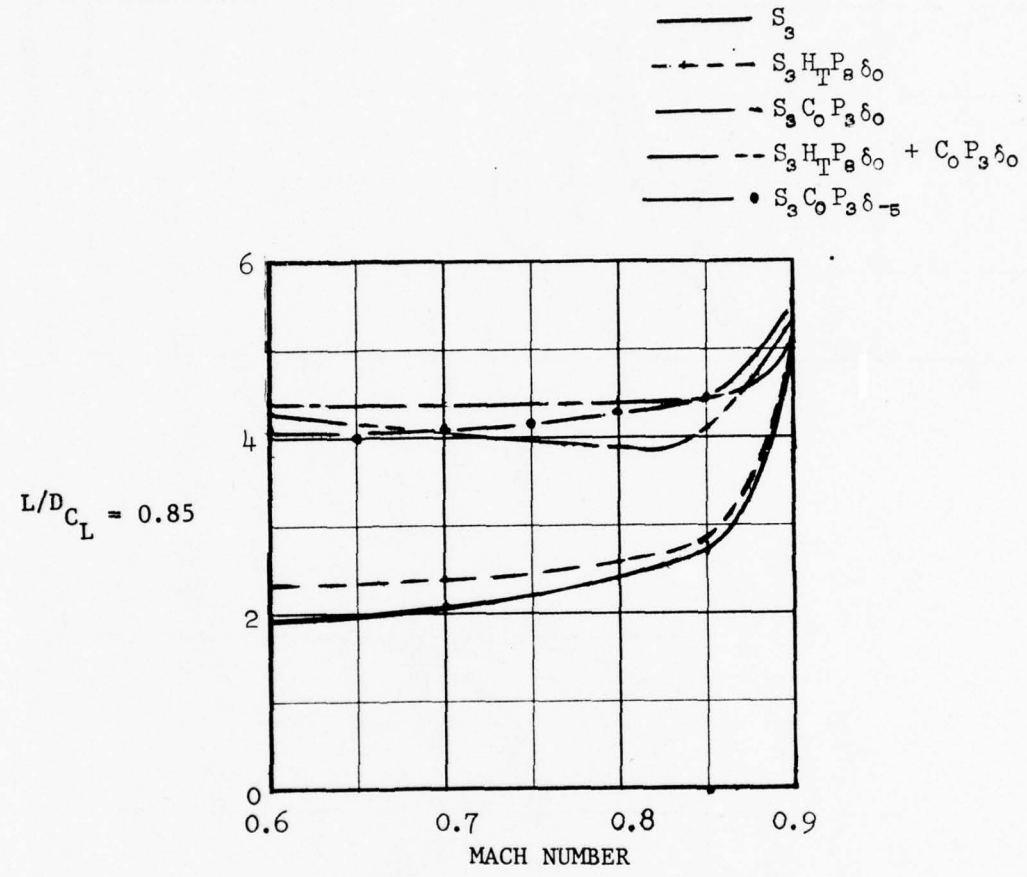

Figure 15 - Variation of Lift-to-Drag Ratios with Mach Number at a Lift Coefficient of 0.85 for Configurations with and without Canards

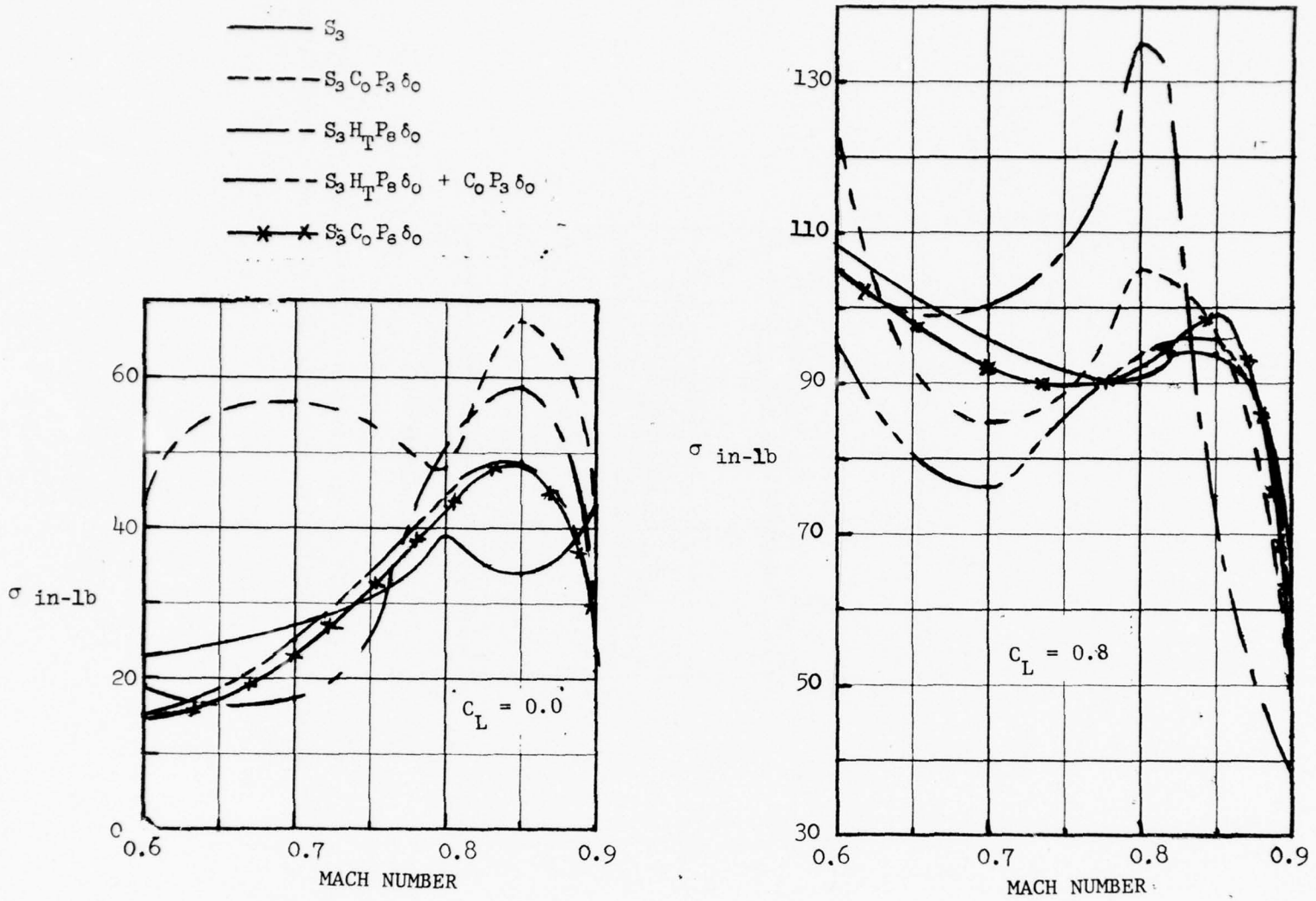

Figure 16 - Variation of Root Mean Square Bending Moment with Mach Number for Several Canard Positions and Deflection Angles for the 25-Degree Sweep Wing

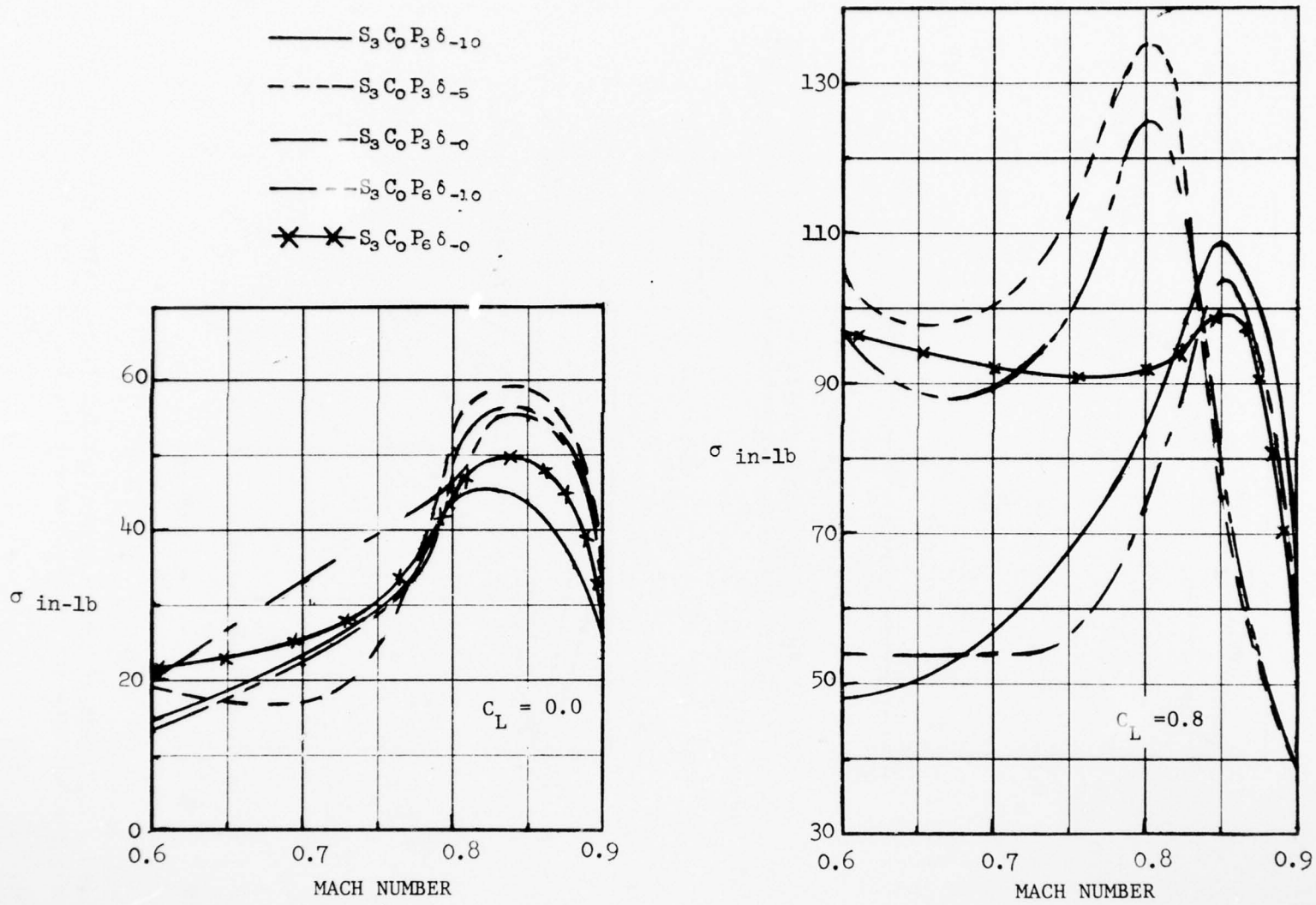

Figure 17 - Variation of Root Mean Square Bending Moment with Mach Number for Configurations with and without Canards for the 25-Degree Sweep Wing.

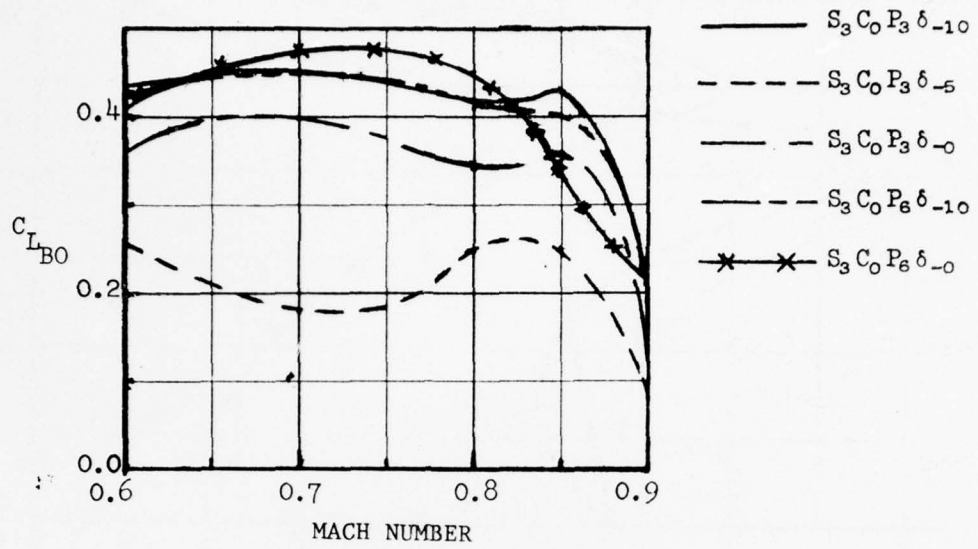

Figure 18 - Variation of Buffet Onset Lift Coefficient with Mach Number for Several Canard Positions and Deflection Angles for the-25 Degree Sweep Wing

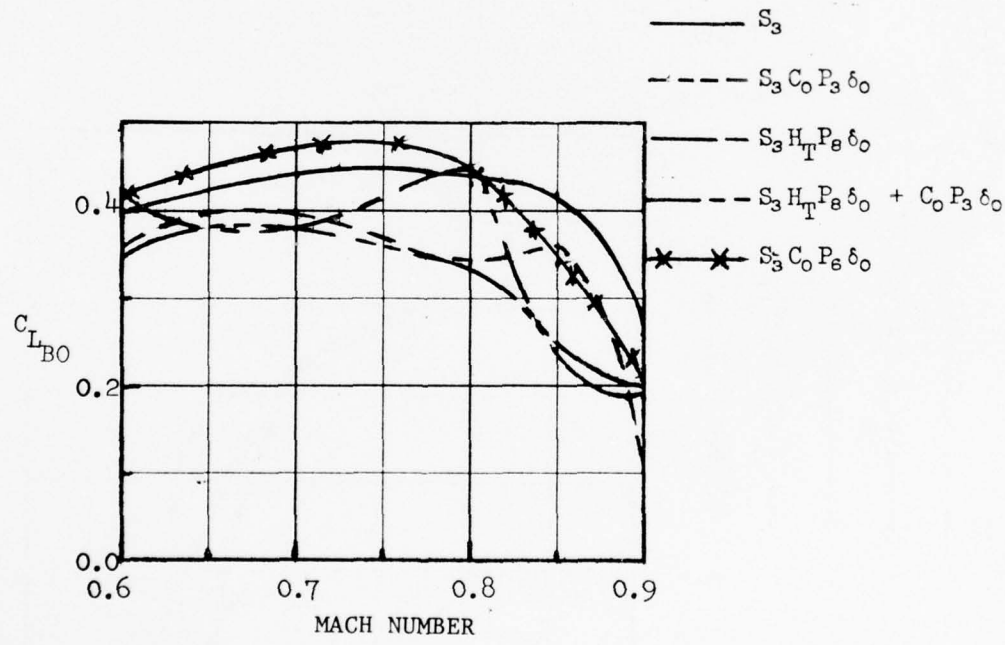

Figure 19 - Variation of Buffet Onset Lift Coefficient with Mach Number for Configurations with and without Canards for the 25-Degree Sweep Wing

Figure 20 - Comparisons of Configuration with and without Canards for the 50-Degree Sweep Wing

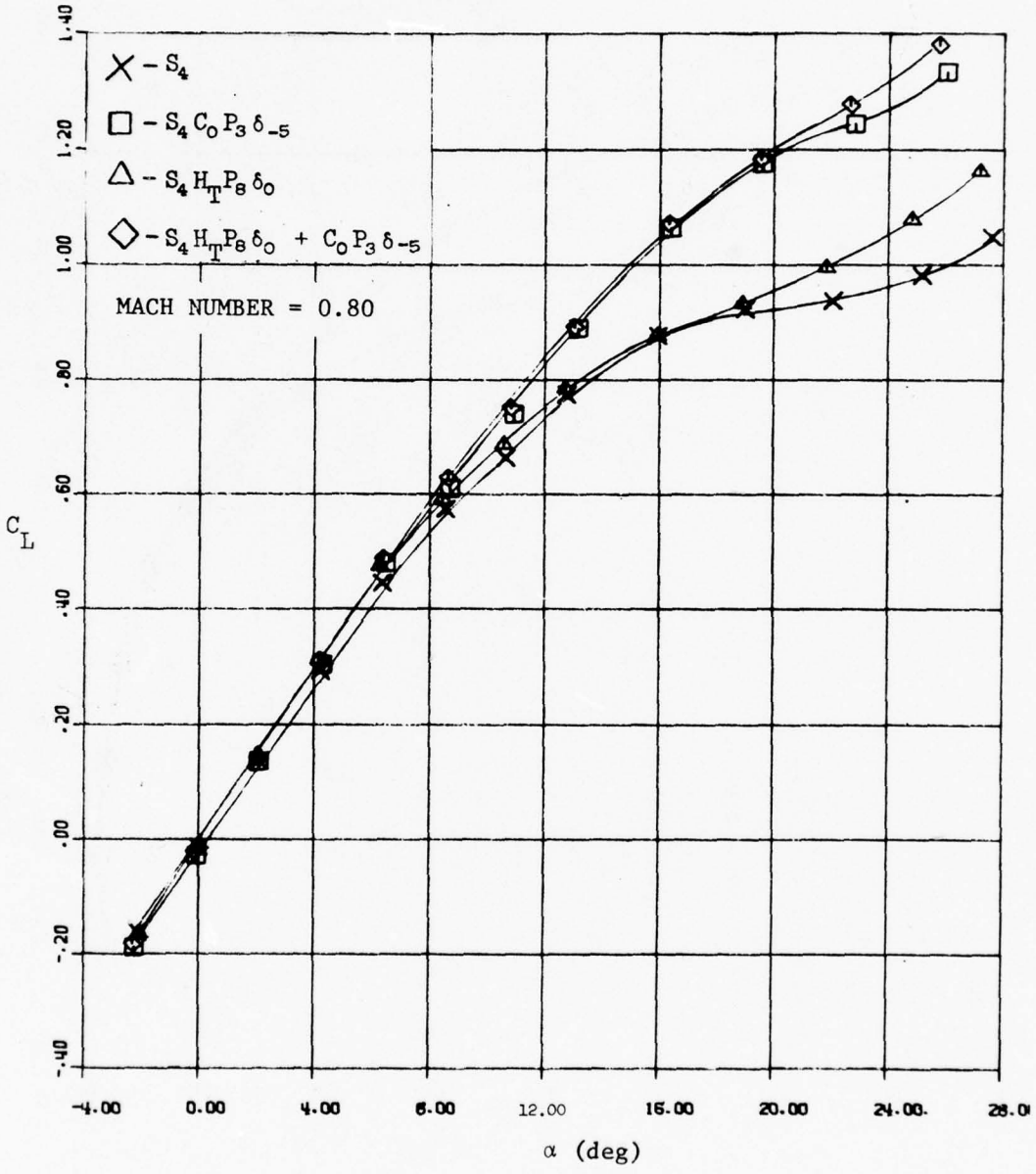

Figure 20a - C_L versus α

Figure 20 (Continued)

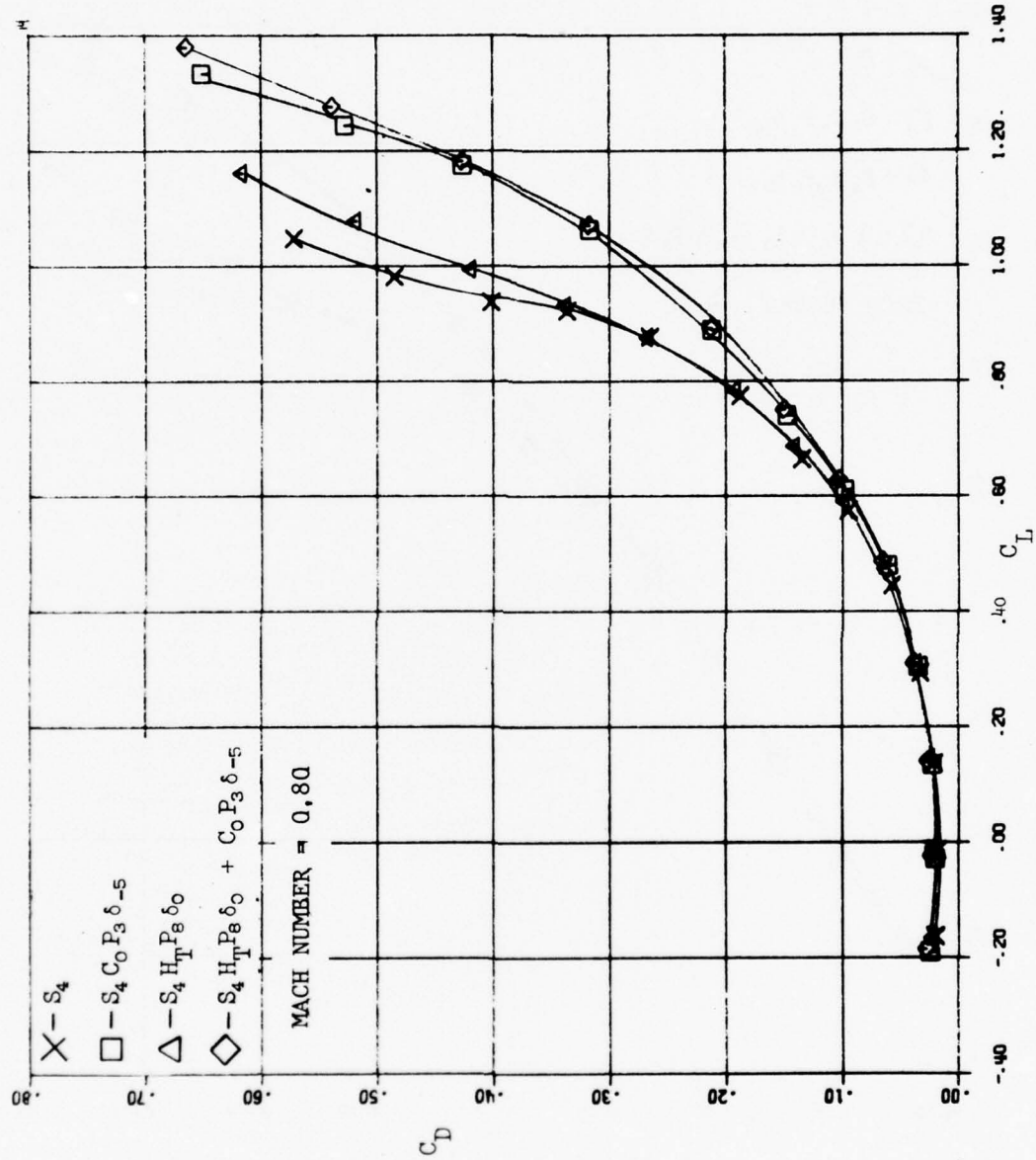

Figure 20b.- C_D versus C_L

Figure 20 (Continued)

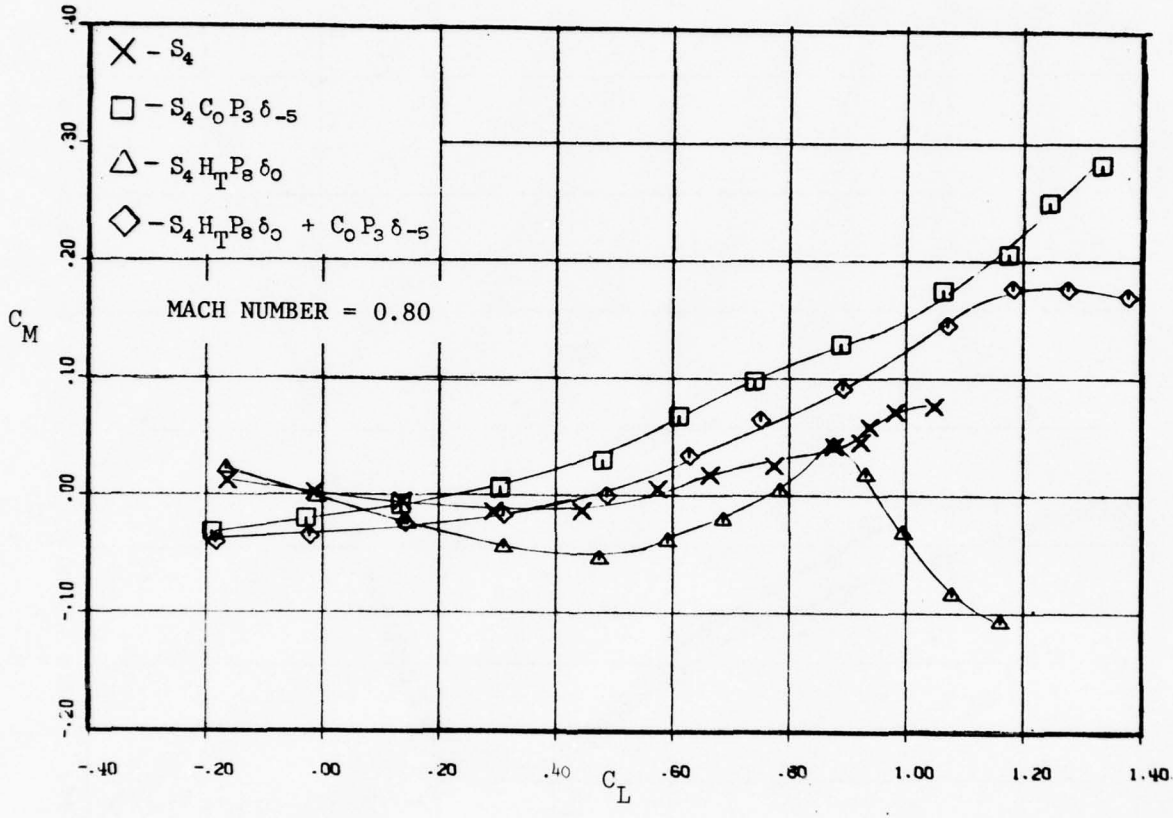

Figure 20c - C_M versus C_L

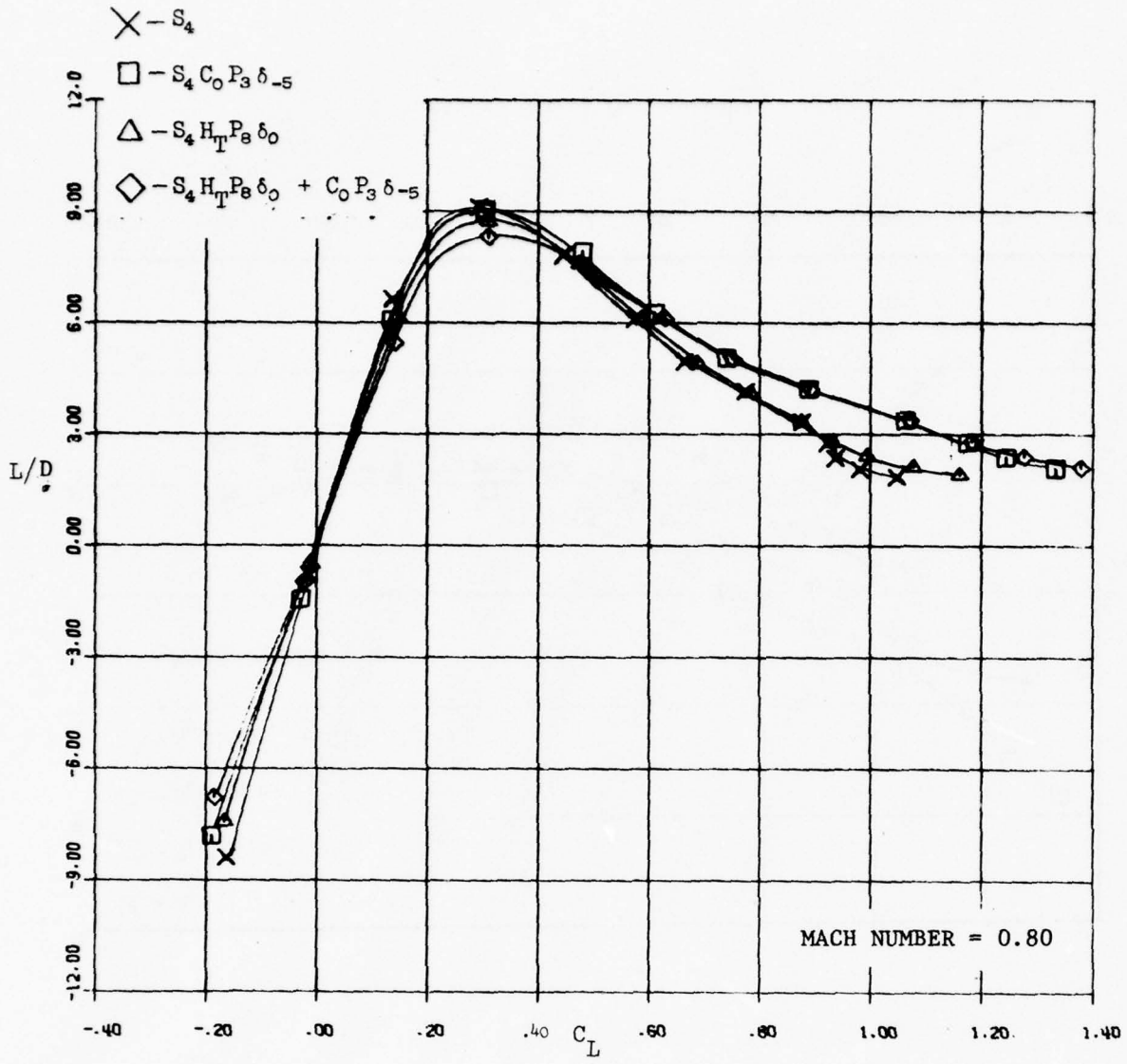

Figure 20d - L/D versus C_L

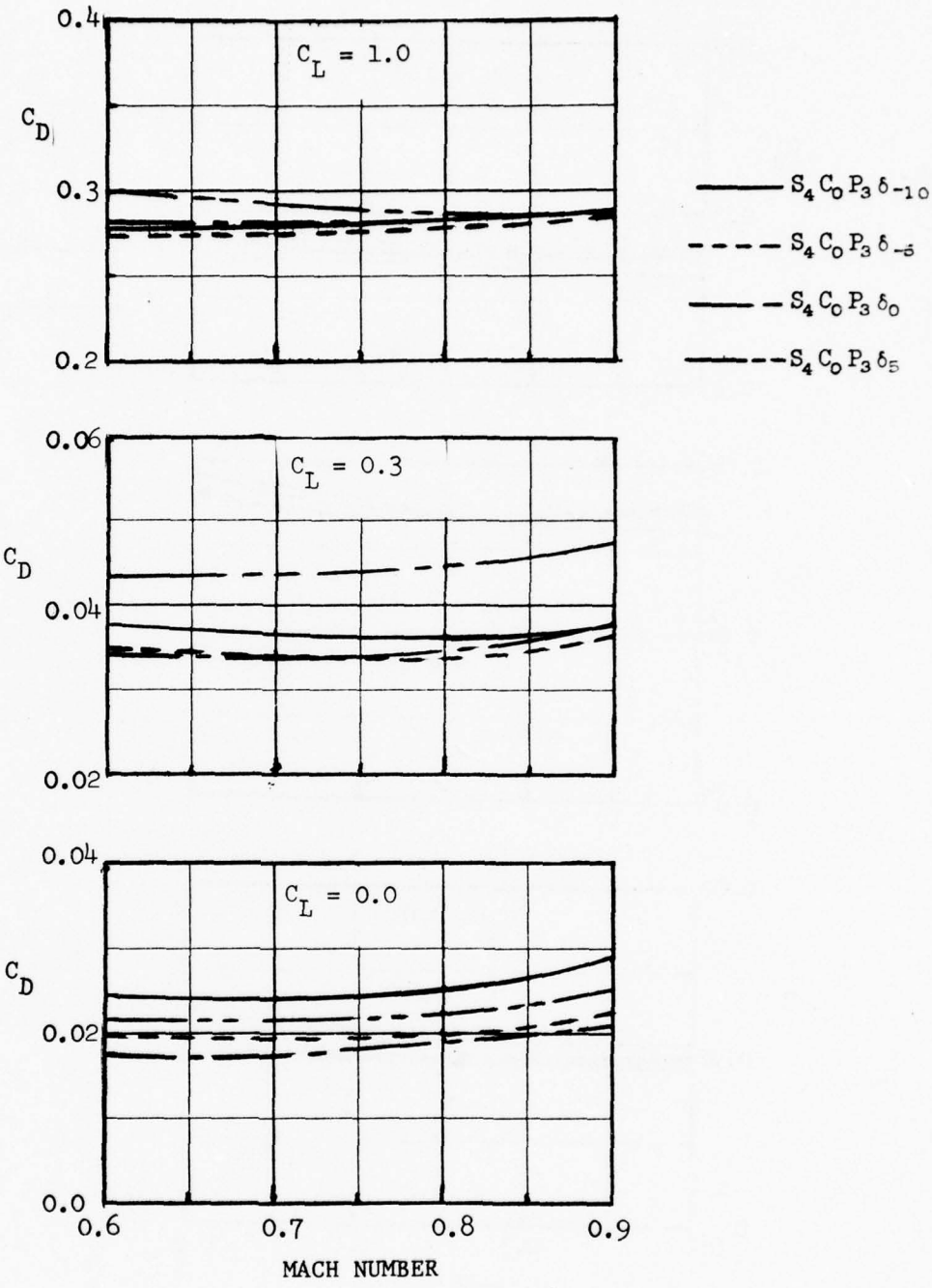

Figure 21 - Effect of Canard Deflection on Drag for the 50-Degree Sweep Wing

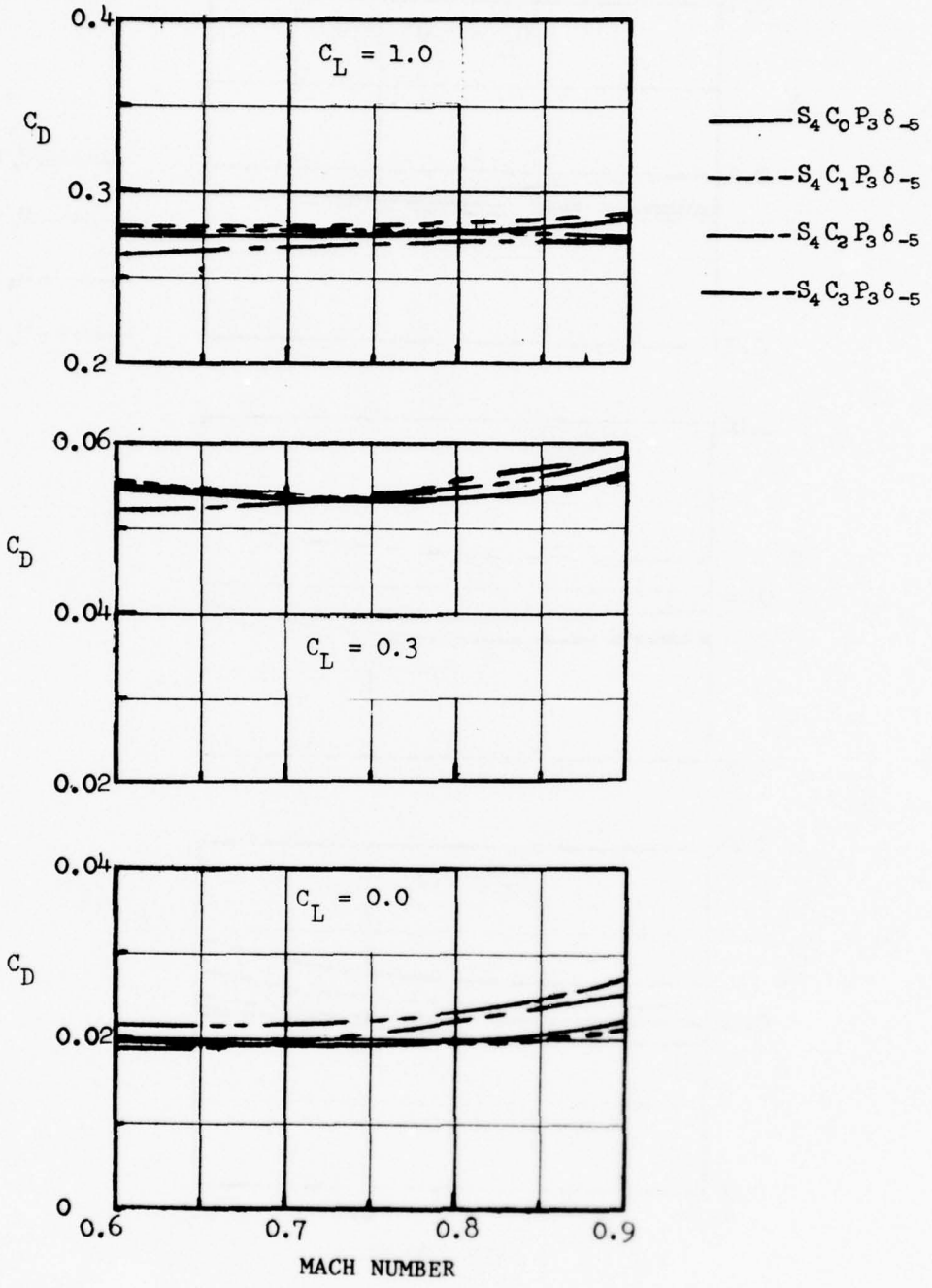

Figure 22 - Effect of Canard Planform on Drag for the 50-Degree Sweep Wing

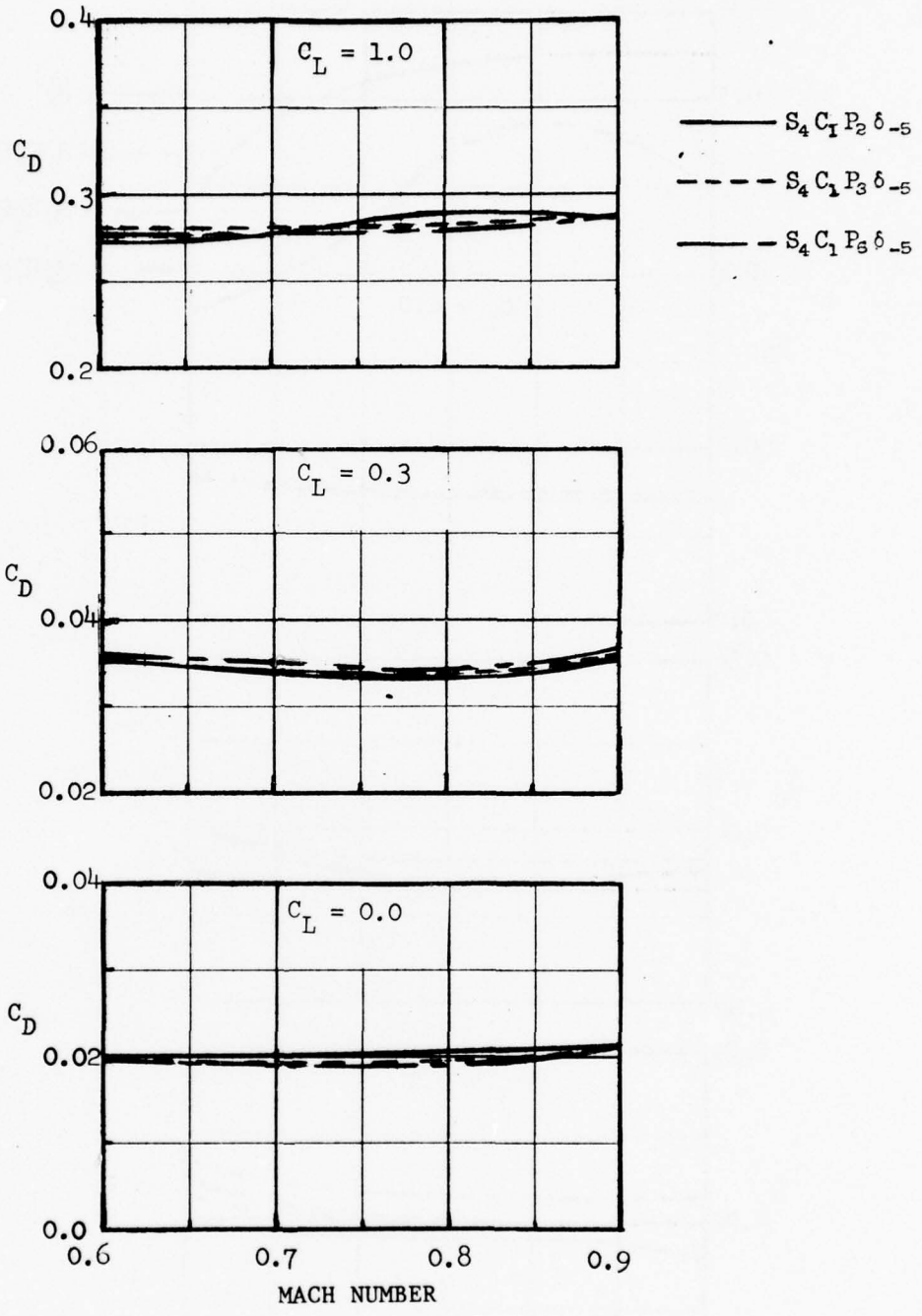

Figure 23 - Effect of Canard Position on Drag for the 50-Degree Sweep Wing

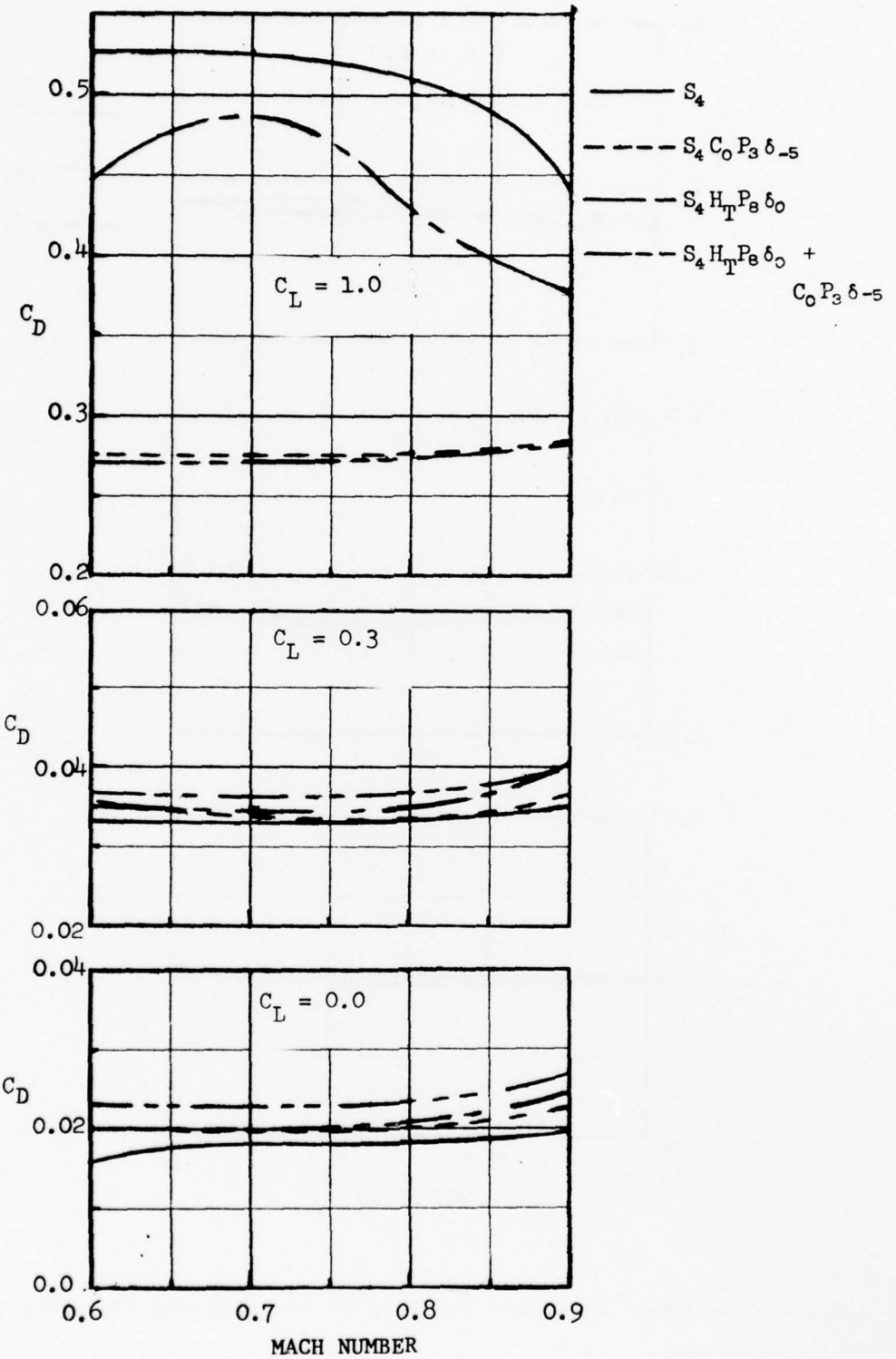

Figure 24 - Comparison of Drag Coefficients for Configurations with and without Canards for the 50-Degree Sweep Wing

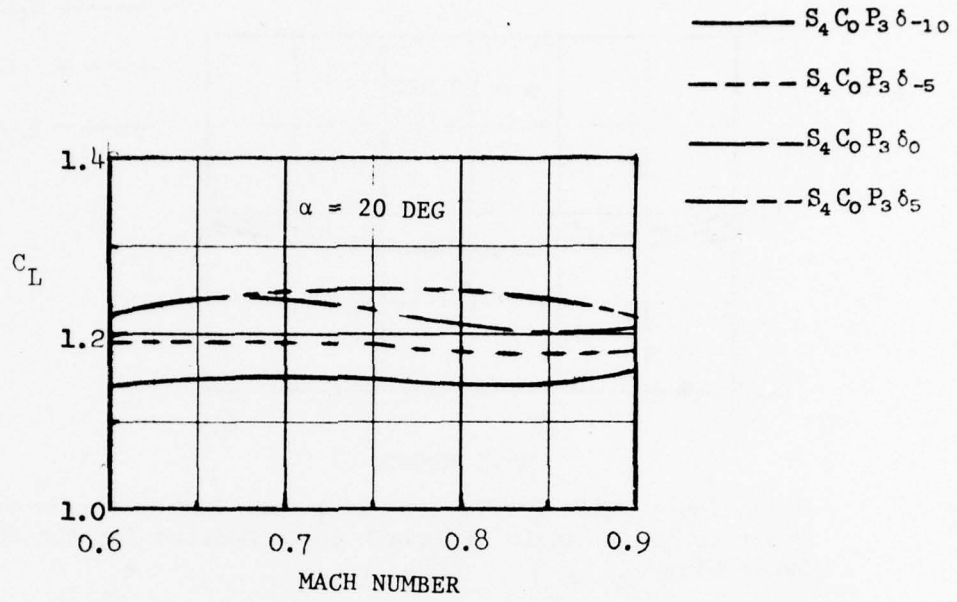

Figure 25 - Variation of Lift Coefficient with Mach Number for Several Canard Deflections at an Angle of Attack of 20 Degrees for the 50 Degree Sweep Wing

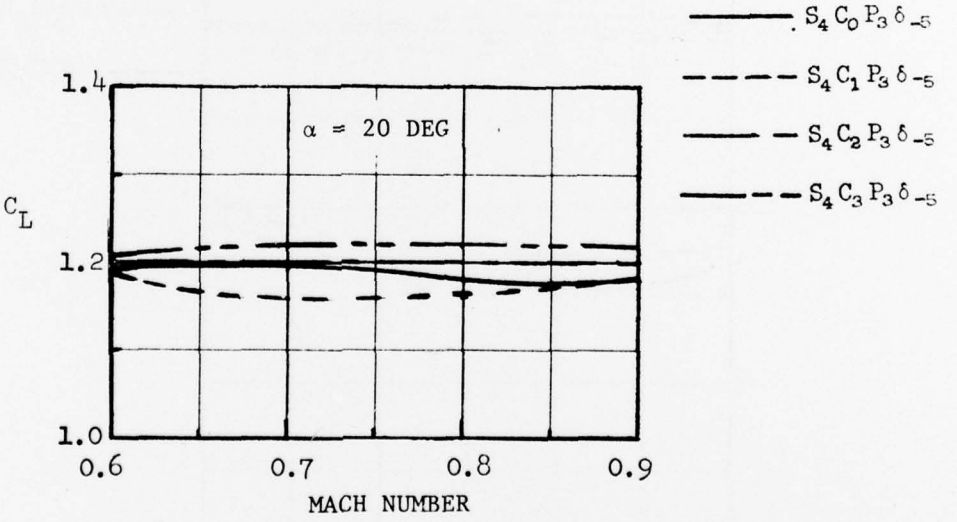

Figure 26 - Variation of Lift Coefficient with Mach Number for Several Canard Planforms at an Angle of Attack of 20 Degrees for the 50-Degree Sweep Wing

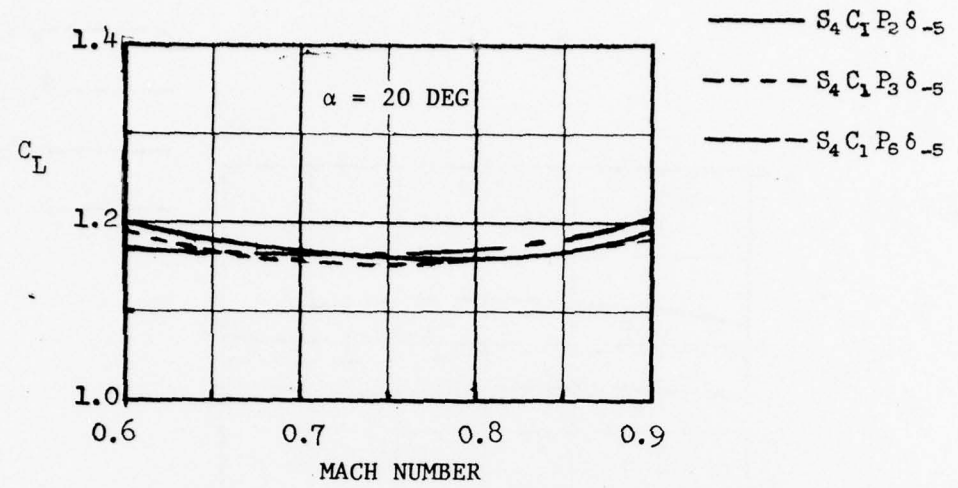

Figure 27 - Variation of Lift Coefficient with Mach Number for Several Canard Positions at an Angle of Attack of 20 Degrees for the 50-Degree Sweep Wing

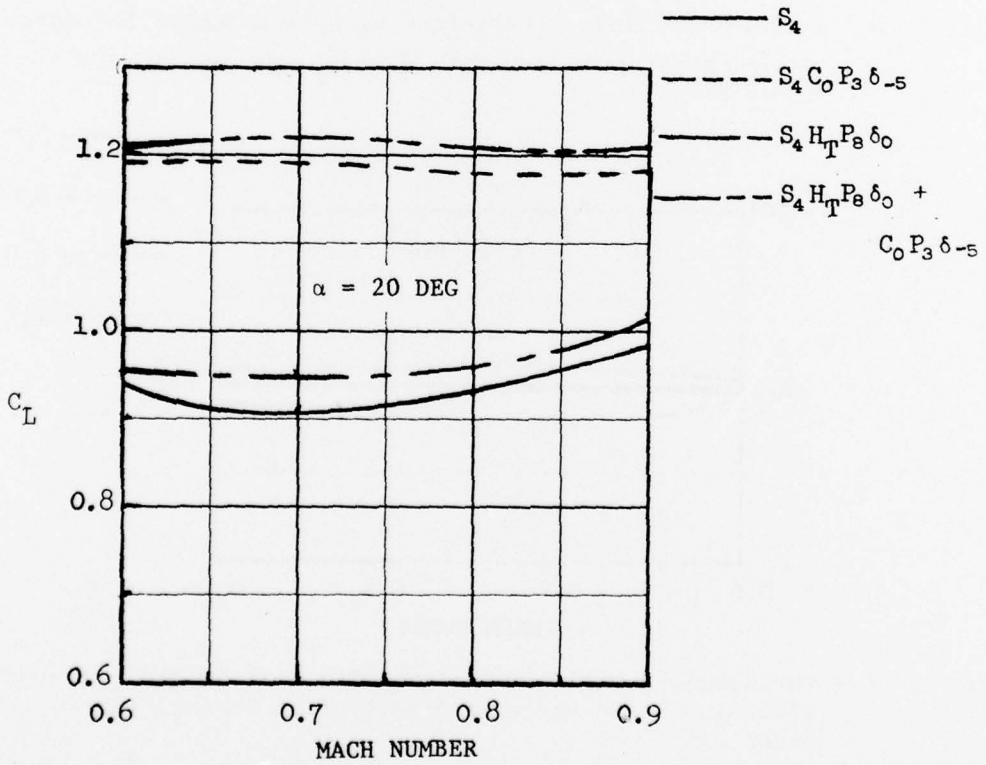

Figure 28 - Variation of Lift Coefficient with Mach Number at an Angle of Attack of 20 Degrees for Configurations with and without Canards for the 50-Degree Sweep Wing

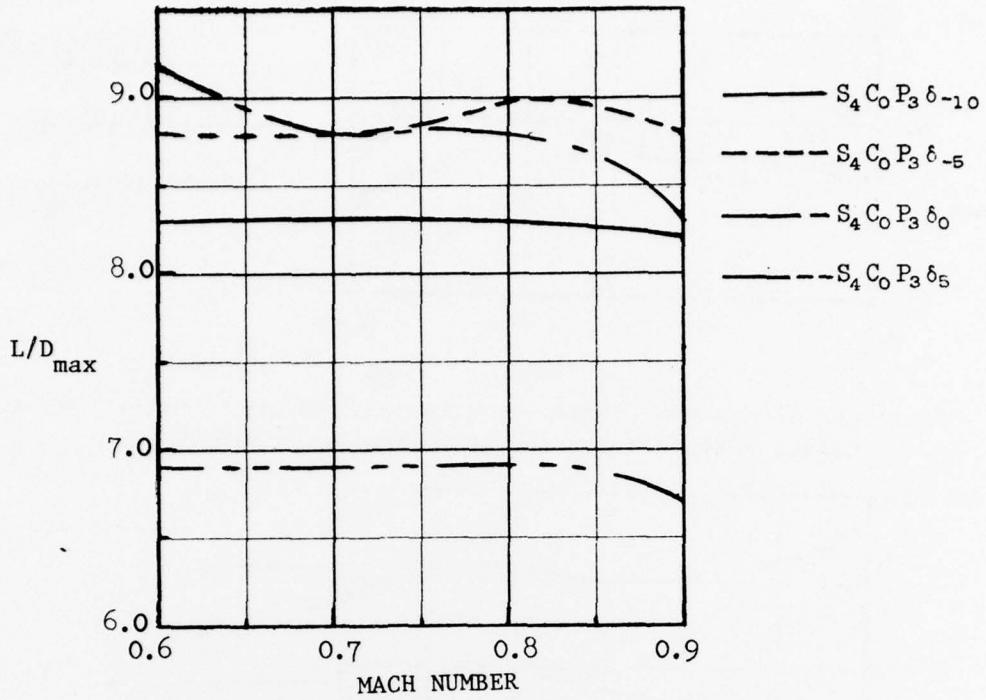

Figure 29 - Variation of Maximum Lift-to-Drag Ratios with Mach Number for Several Canard Deflections for the 50-Degree Sweep Wing

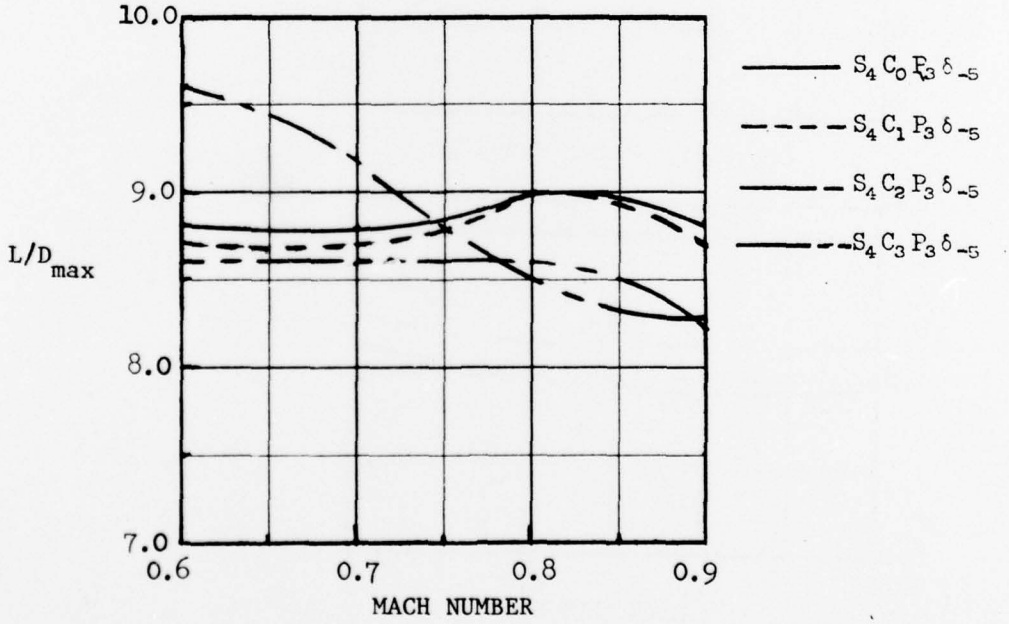

Figure 30 - Variation of Maximum Lift-to-Drag Ratios with Mach Number for Several Canard Planforms for the 50-Degree Sweep Wing

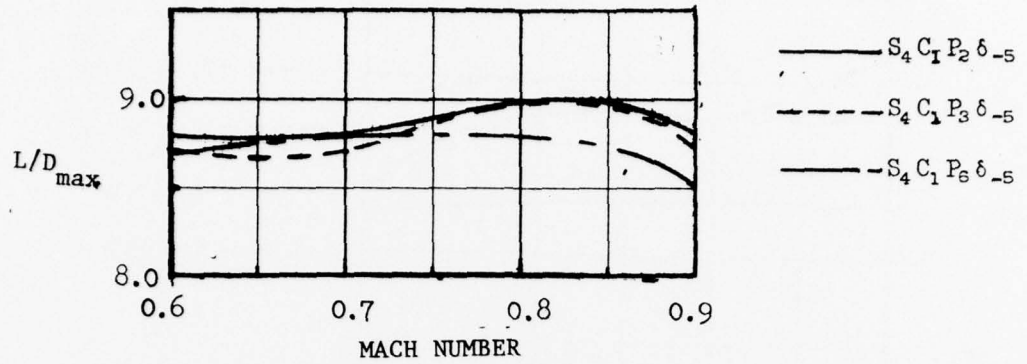

Figure 31 - Variation of Maximum Lift-to-Drag Ratios with Mach Number for Several Canard Positions for the 50-Degree Sweep Wing

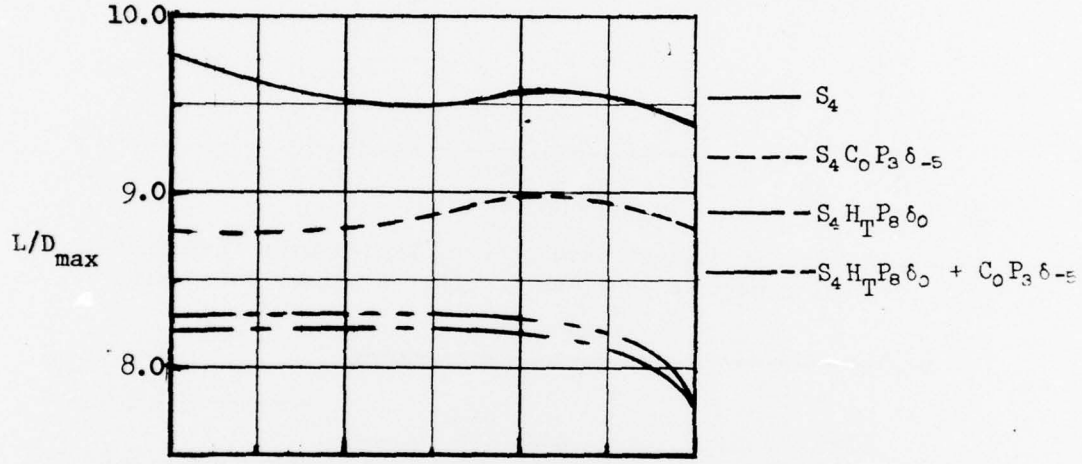

Figure 32a - MAXIMUM L/D

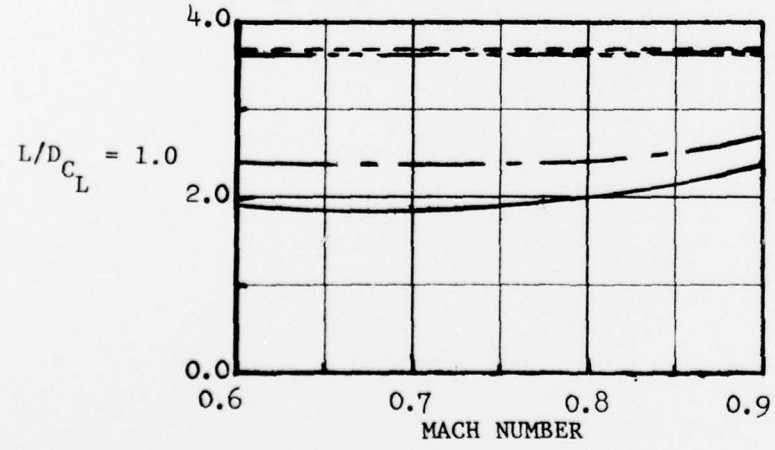

Figure 32b - L/D at $C_L = 1.0$

Figure 32 - Variation of Lift-to-Drag Ratios with Mach Number for Configurations with and without Canards for the 50-Degree Sweep Wing

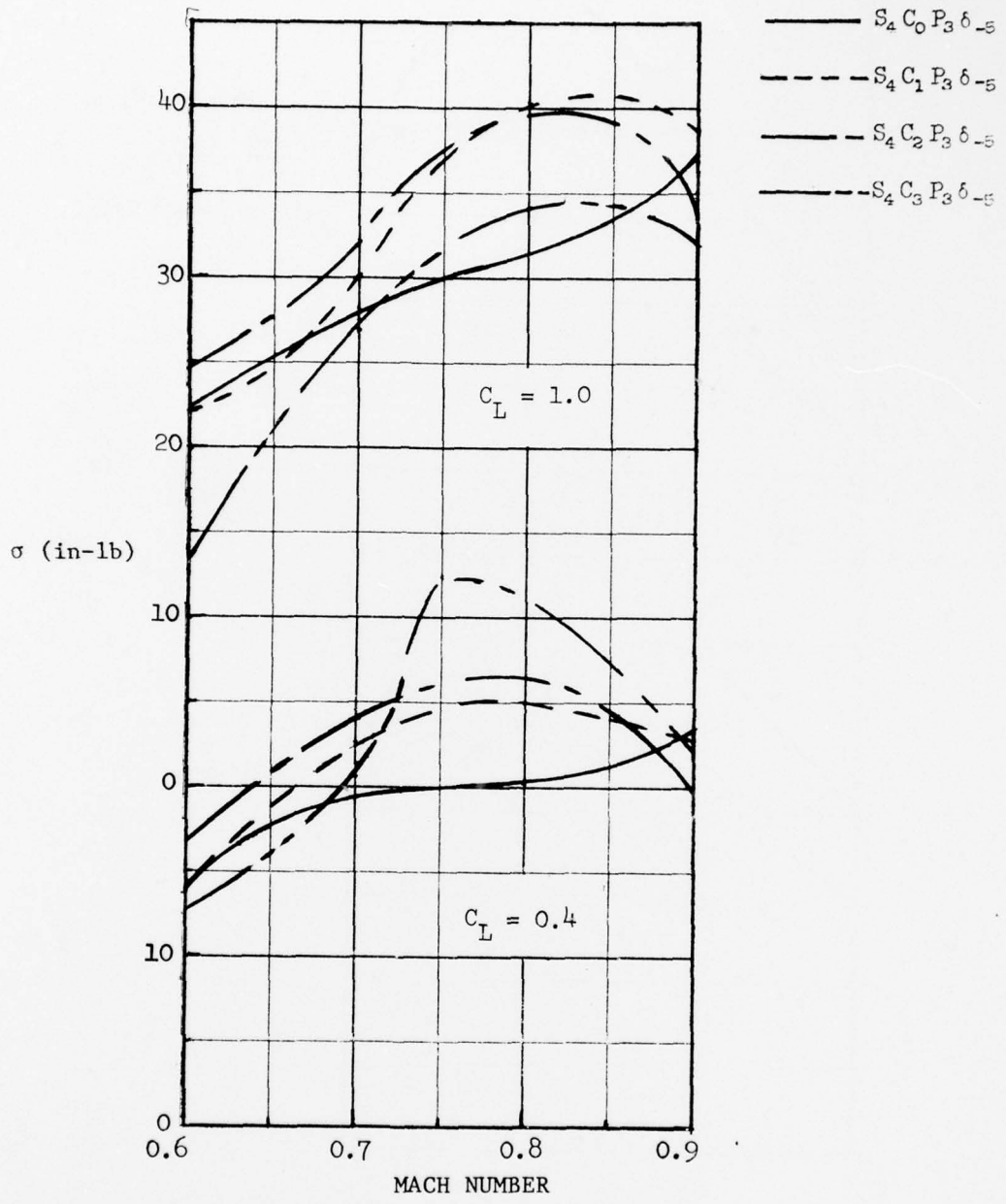

Figure 33 - Variation of Root Mean Square Bending Moment with Mach Number for Several Canard Planforms for the 50-Degree Sweep Wing

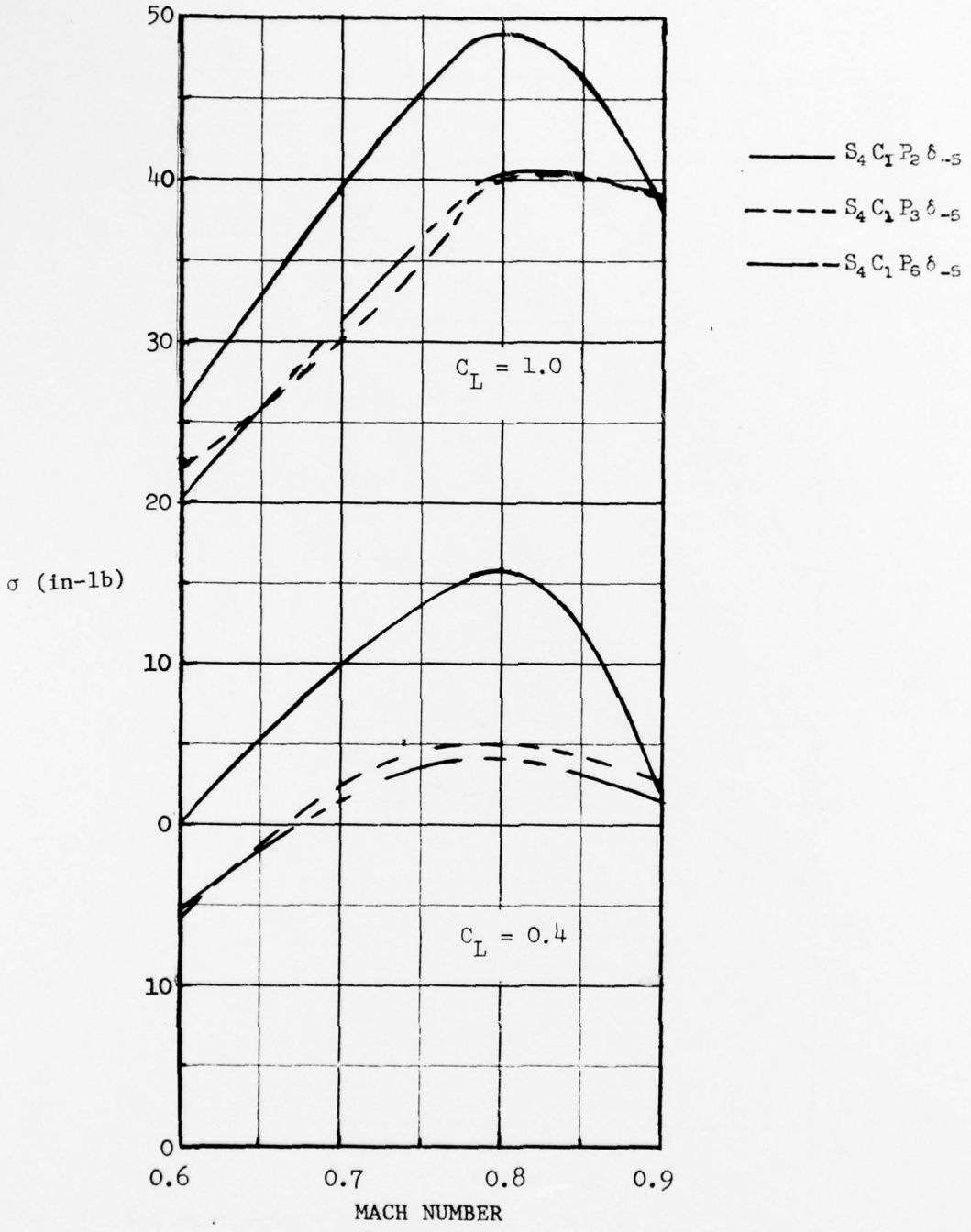

Figure 34 - Variation of Root Mean Square Bending Moment with Mach Number for Several Canard Positions for the 50-Degree Sweep Wing

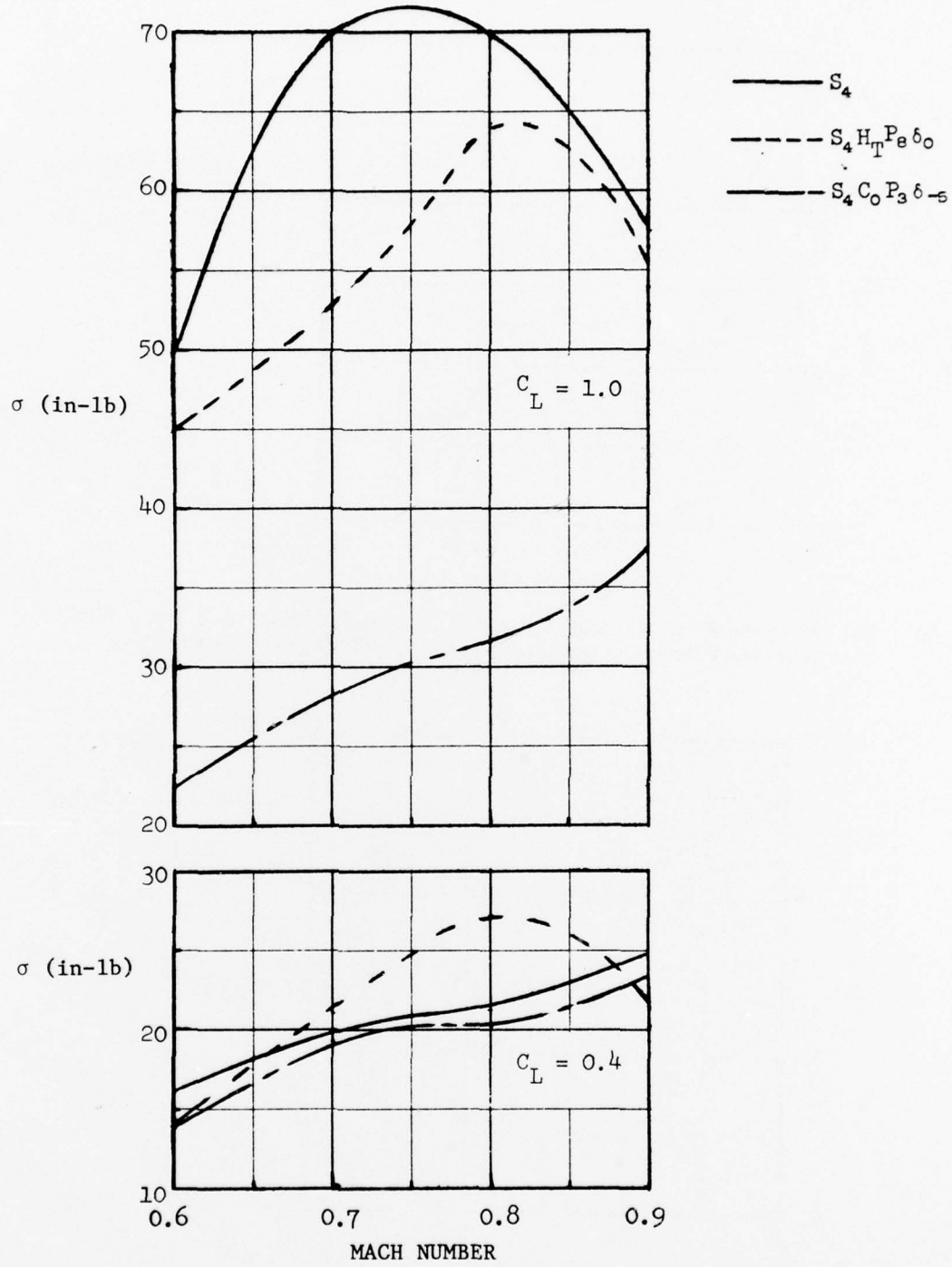

Figure 34 - Variation of Root Mean Square Bending Moment with Mach Number for Configurations with and without Canards for the 50-Degree Sweep Wing

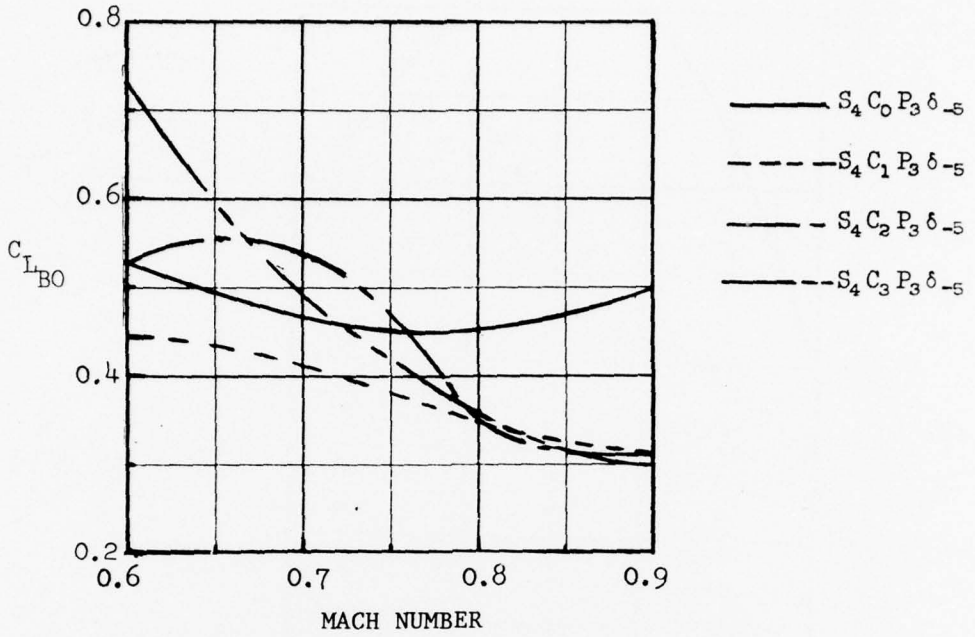

Figure 36 - Variation of Buffet Onset Lift Coefficient with Mach Number for Various Canard Planforms for the 50-Degree Sweep Wing

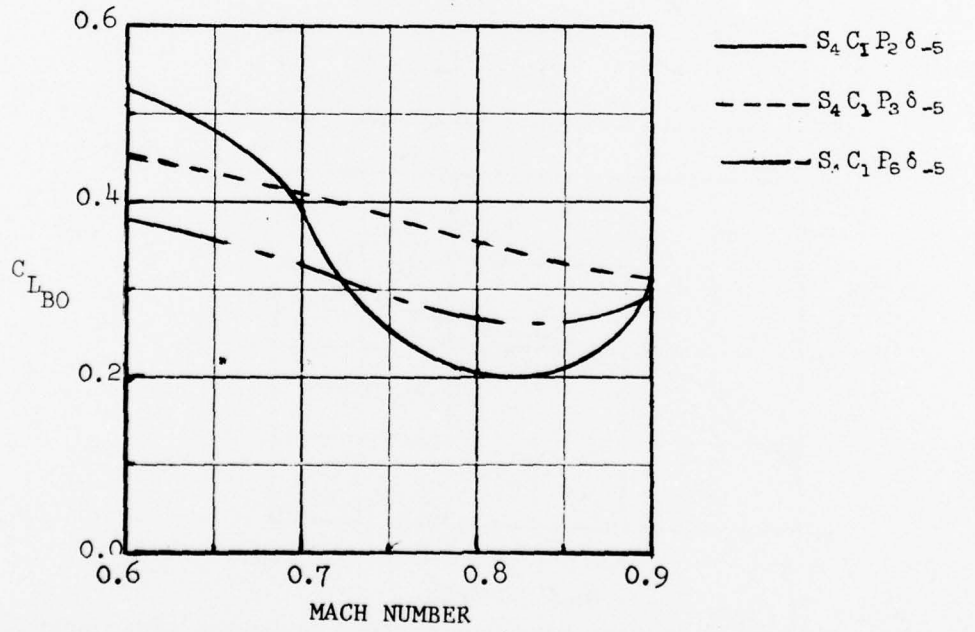

Figure 37 - Variation of Buffet Onset Lift Coefficient with Mach Number for Several Canard Positions for the 50-Degree Sweep Wing

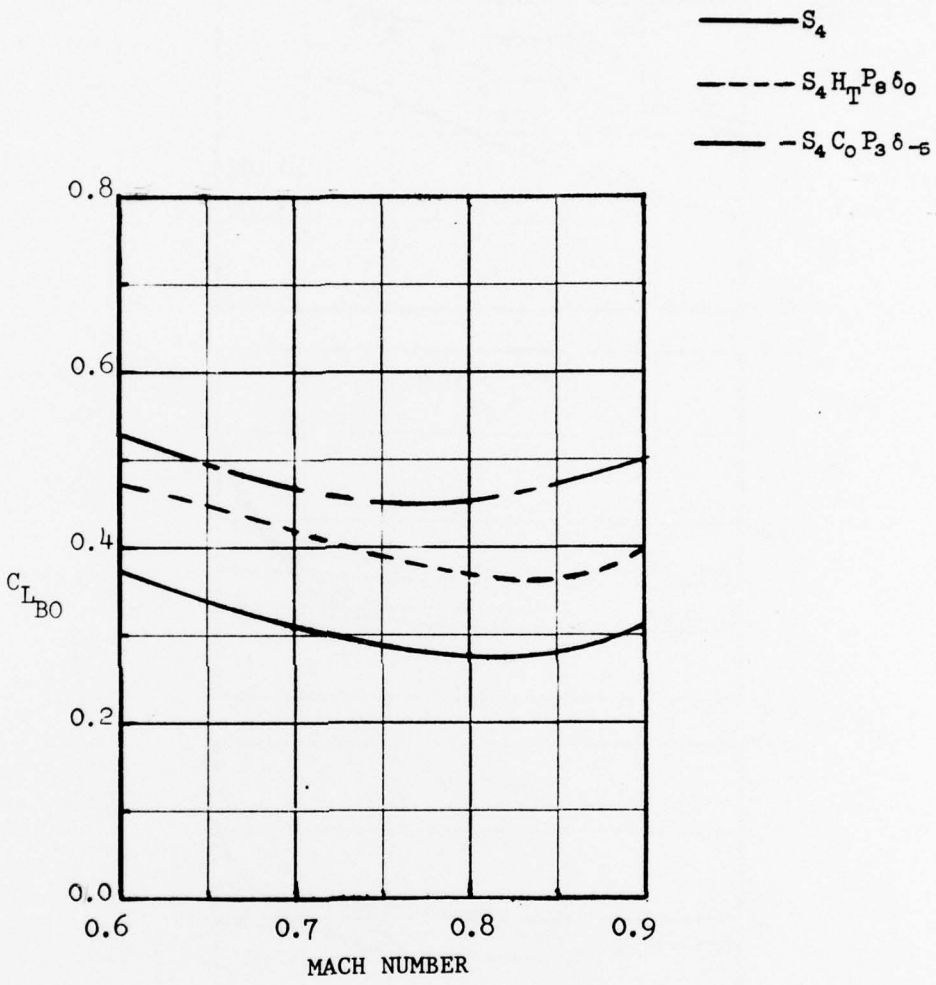

Figure 38 - Variation of Buffet Onset Lift Coefficient with Mach Number for Configurations with and without Canards for the 50-Degree Sweep Wing

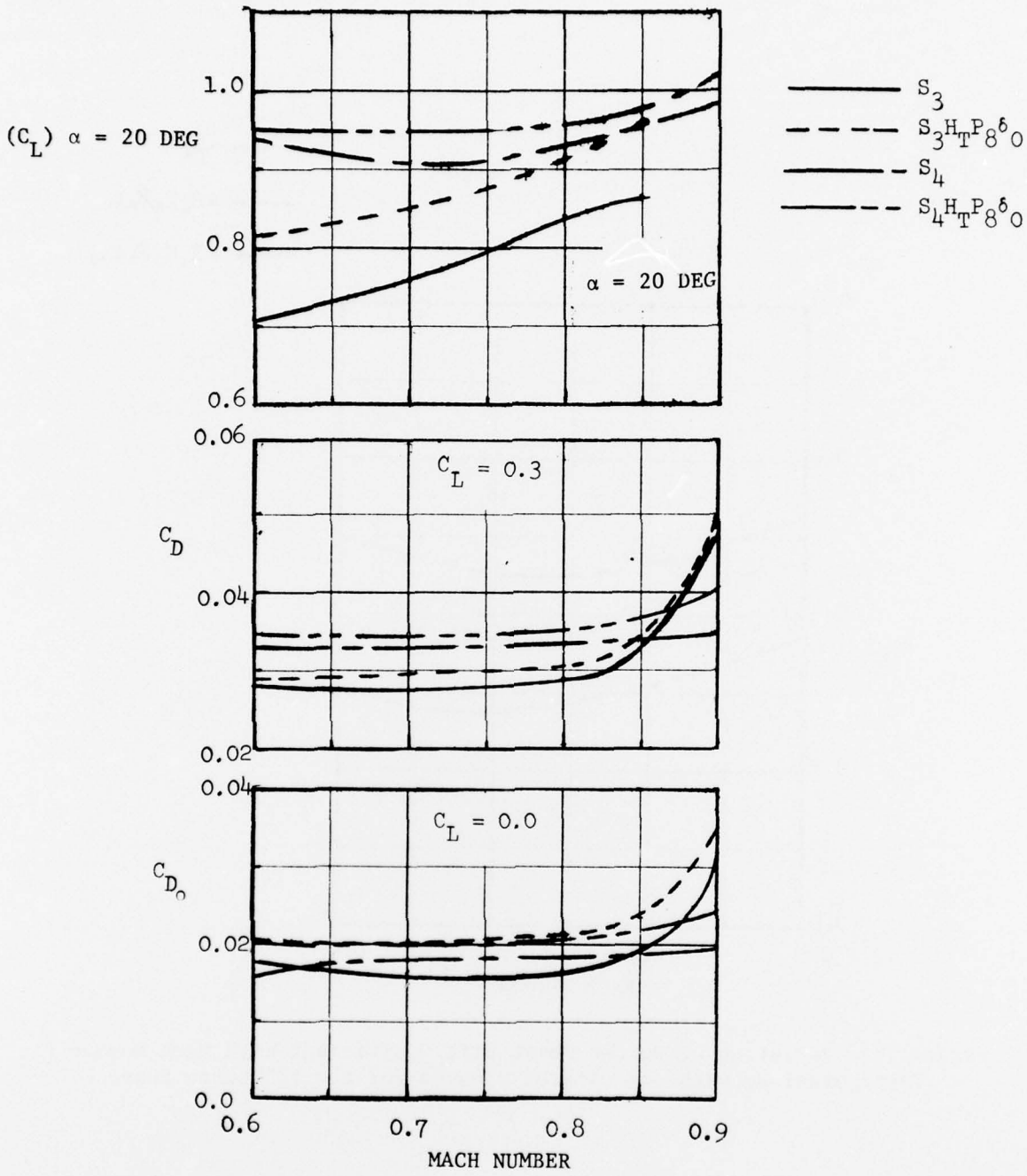

Figure 39 - Comparison of Lift and Drag for the 25-and 50-Degree Sweep Wings as a Function of Mach Number

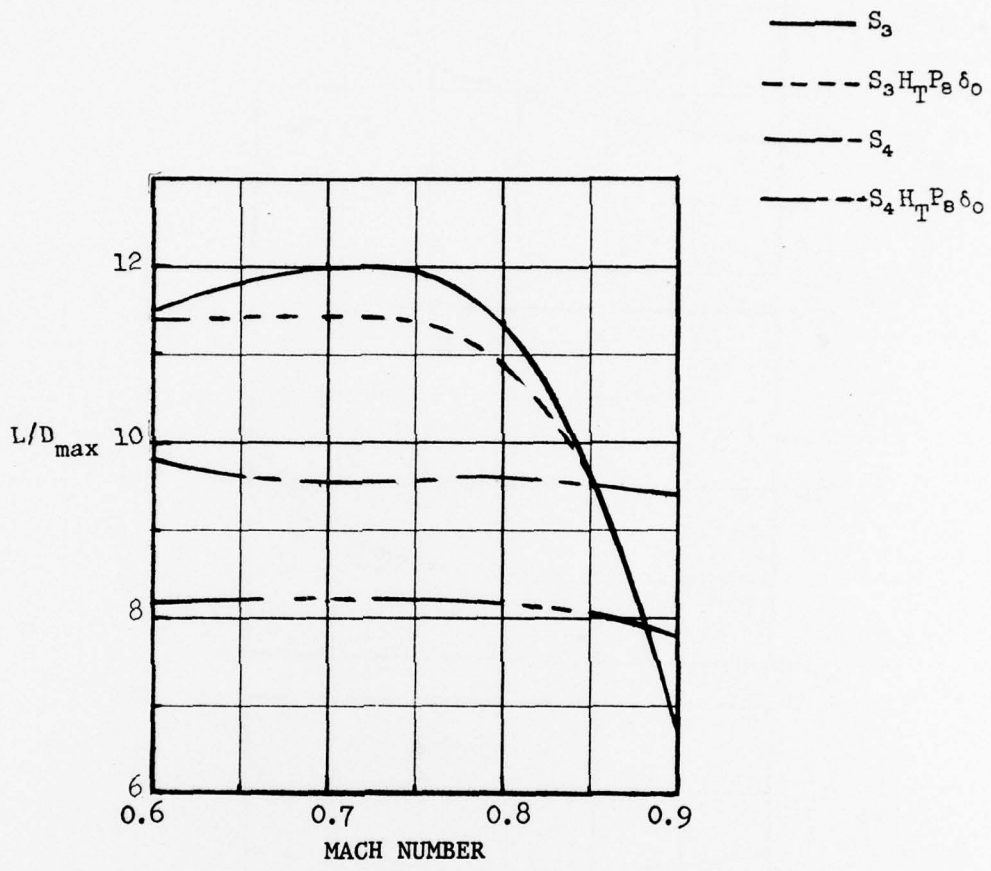

Figure 40 - Comparison of Maximum Lift-to-Drag Ratios for the 25- and 50-Degree Sweep Wings as a Function of Mach Number

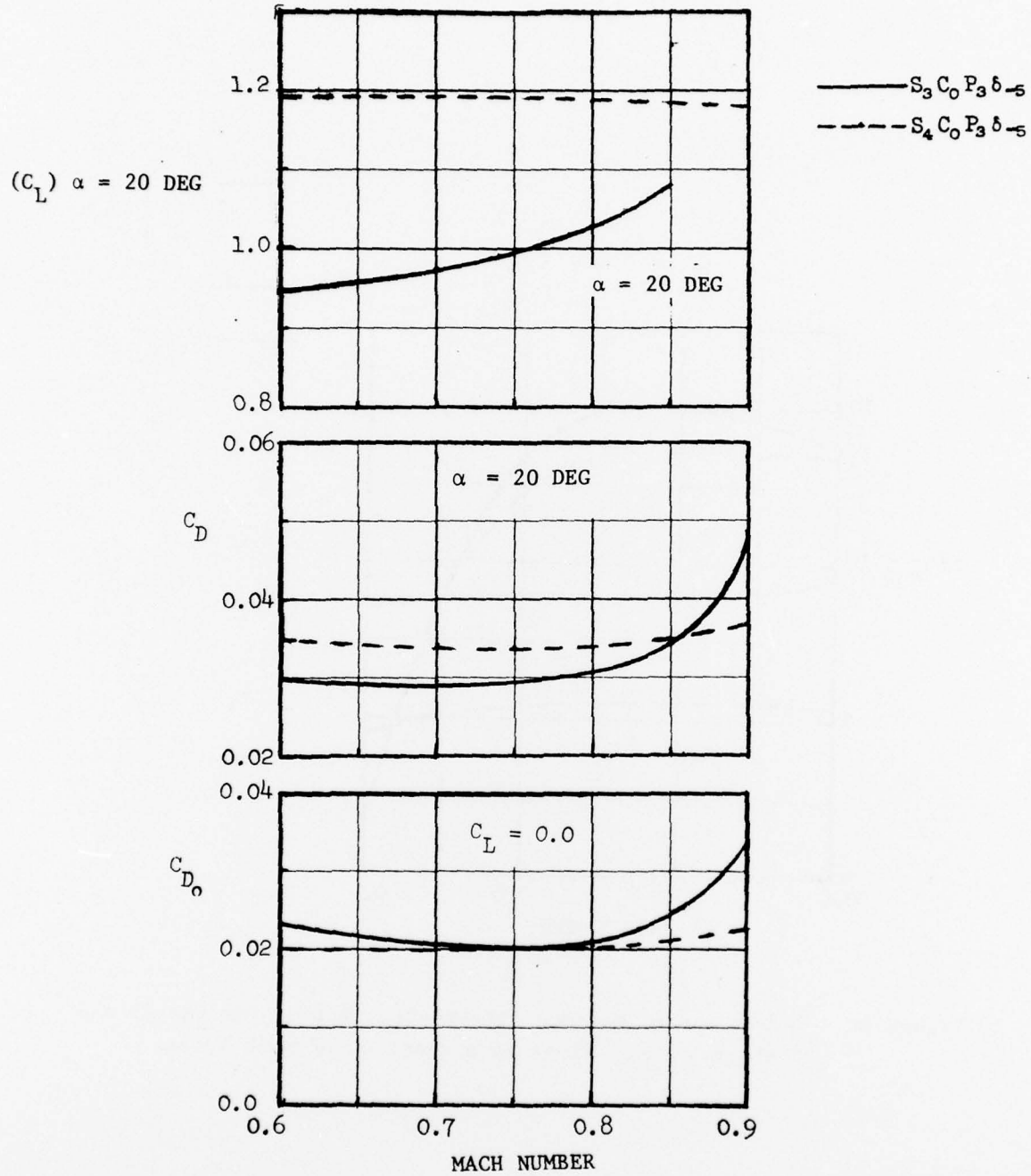

Figure 41 - Comparison of Lift and Drag for the Identical Canard Mounted on the 25-and 50-Degree Sweep Wing Configurations

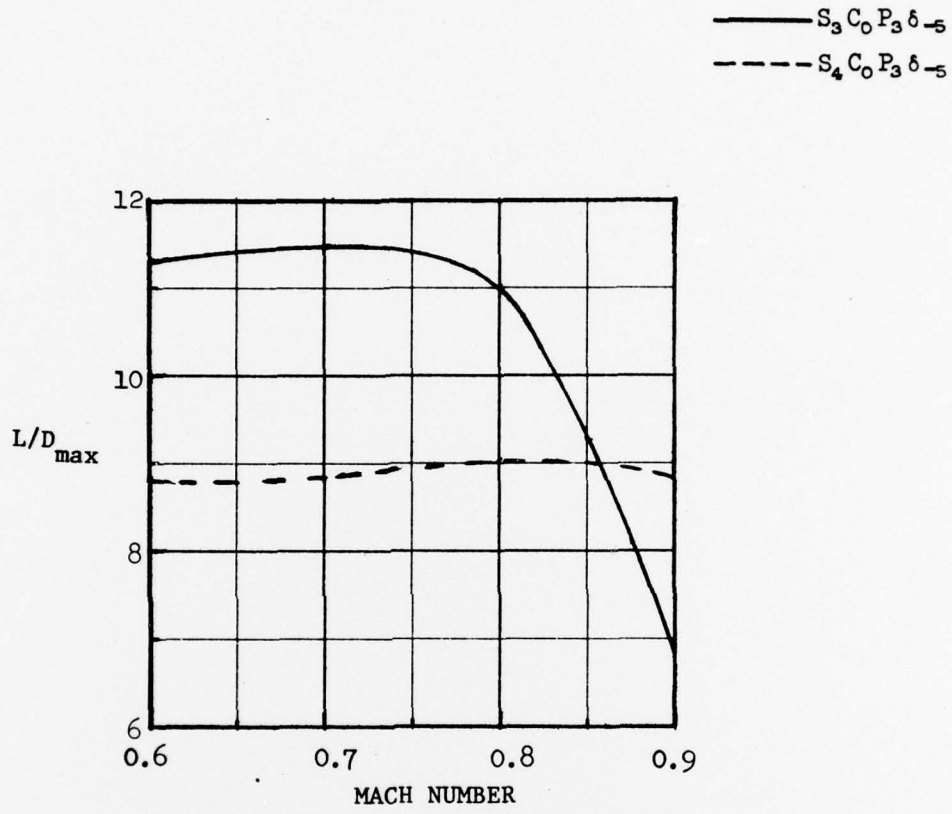

Figure 42 - Comparison of the Maximum Lift-to-Drag Ratios for the Identical Canard Mounted on the 25-and 50-Degree Wing Configurations

DTNSRDC ISSUES THREE TYPES OF REPORTS

(1) DTNSRDC REPORTS, A FORMAL SERIES PUBLISHING INFORMATION OF PERMANENT TECHNICAL VALUE, DESIGNATED BY A SERIAL REPORT NUMBER.

(2) DEPARTMENTAL REPORTS, A SEMIFORMAL SERIES, RECORDING INFORMATION OF A PRELIMINARY OR TEMPORARY NATURE, OR OF LIMITED INTEREST OR SIGNIFICANCE, CARRYING A DEPARTMENTAL ALPHANUMERIC IDENTIFICATION.

(3) TECHNICAL MEMORANDA, AN INFORMAL SERIES, USUALLY INTERNAL WORKING PAPERS OR DIRECT REPORTS TO SPONSORS, NUMBERED AS TM SERIES REPORTS; NOT FOR GENERAL DISTRIBUTION.